1ST INTERNATIONAL CONFERENCE ON PHONONIC CRYSTALS, METAMATERIALS & OPTOMECHANICS

Extended Abstracts

Track 4: Phonon Transport

Phononics 2011: First International Conference on Phononic Crystals, Metamaterials and Optomechanics
Santa Fe, New Mexico, USA, May 29-June 2, 2011
PHONONICS-2011-0022

Band-gap Acoustic States in 1D and 2D Single Layer Graphene Sheet Systems

Fabrizio Scarpa[1] , **Massimo Ruzzene**[2]

[1] *ACCIS, University of Bristol, BS8 1TR Bristol, UK, f.scarpa@bris.ac.uk,*
[2] *D. Guggenheim School of Aerospace Engineering, Georgia Institute of Technology, Atlanta, GA 30332. massimo.ruzzene@ae.gatech.edu*

Abstract: We evaluate the pass-stop band characteristics of mechanical wave propagating in periodic nanostructures made with nanoribbons or graphene sheets with non-reconstructed defects..

In this work we study the acoustic wave propagation and band-gap characteristics in 1D and 2D single layer graphene sheets with periodic boundary conditions. The 1D graphene systems are represented by graphene nanoribbons with periodic clamped conditions (bridges). The calculation of the wave dispersion characteristics is performed using an atomistic-FE method where the equivalent properties of the C-C bonds [1,2], considered as structural beams, are computed through the minimisation of the Hamiltonian of the system for a specific set of wave propagation constants [3]. The graphene sheets are assembled using the classical FE techniques relative to truss structures, while the pass-stop band characteristics calculated using methods developed by the Authors for periodic 1D and 2D beam assemblies. The periodic graphene nanoribbons show specific wave dispersion properties depending on the edges (zigzag or armchair) along which the acoustic waves are propagating. From a mechanical perspective, the edges of the finite graphene nanoribbons induce a global mechanical special orthotropy of the nanostructures, justifying the assumption that any beam-like wave dispersions could be represented using different Young's moduli along the various directions. We explore also the possibility of nanophononics patterns [4] using periodic non-reconstructed vacancies (NRVs), or assemble graphene sheets with cross-rectangular geometry. The periodic nanostructures provide phase constant surface characteristics, which can used to design novel generation of photonics devices with high GHz bands.

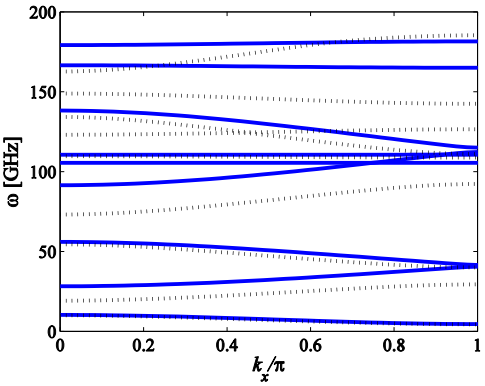

Figure 1. Wave dispersion characteristics for a zigzag (8,0) nanoribbon in minimised (continuous) and non-minimised configuration.

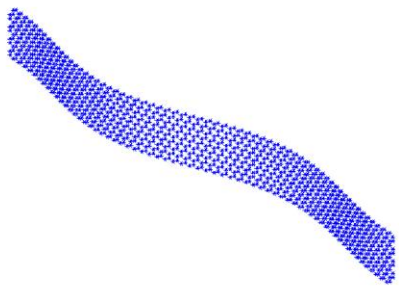

Figure 2 2nd modeshape for the propagation constant kx (0,π) in 1D wave propagation of a nanoribbon.

Phononics 2011: First International Conference on Phononic Crystals, Metamaterials and Optomechanics
Santa Fe, New Mexico, USA, May 29-June 2, 2011
PHONONICS-2011-0022

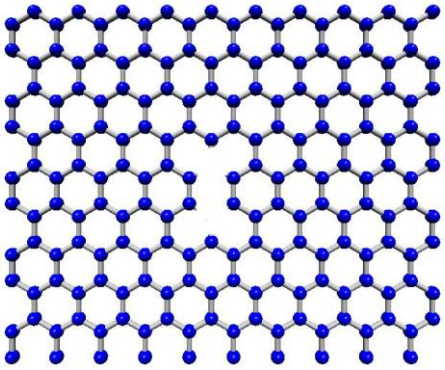

Figure 4. Unit element with double NRV for a 2D periodic array of graphene sheets

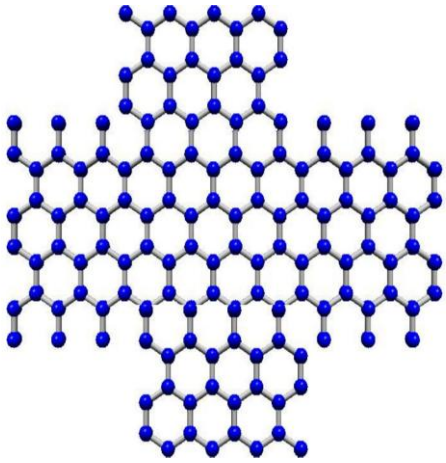

Figure. 5. Periodic unit of assembled (10,0) and (4,0) graphene sheets.

References

[1] Scarpa F, Adhikari S, Srikantha Phani A, 2009. *Nanotechnology*, 20, 065709 (11pp)
[2] Scarpa F, Boldrin L, Peng H X, Remillat C D L, Adhikari S, 2010. *App. Phys. Lett*. 97, 0345012.
[3] Scarpa F, Ruzzene M, Adhikari S, Kam K, 2010. Proceedings of SPIE, San Diego, CA, 6-10 March
[4.] Spadoni A, Ruzzene M, Gonella S and Scarpa F., 2009. *Wave Motion*, 46(7), 435

Phononics 2011: First International Conference on Phononic Crystals, Metamaterials and Optomechanics
Santa Fe, New Mexico, USA, May 29-June 2, 2011
PHONONICS-2011-0042

Phononics: a new science and technology in processing information and controlling heat flow by phonons

Baowen Li[1,2]

[1] *NUS Graduate School for Integrative Sciences and Engineering, Singapore 117456, Singapore*
[2] *Department of Physics, National University of Singapore, Singapore 117542, Singapore*
phylibw@nus.edu.sg

Abstract: Heat due to lattice vibration – *phonons*- is usually regarded as harmful for information processing. However, studies in recent years have changed this mindset. In this paper, I will demonstrate via numerical simulation, theoretical analysis and experiments that, phonons, can be manipulated like electrons. They can be used to carry and process information. Basic phononic devices such as thermal diode, thermal transistor, thermal logic gate and thermal memory can be worked via nonlinear lattice and/or low dimensional nanostructures such as nanowire, nanotube, graphen nanoribbon etc. .

Heat conduction and electric conduction are two fundamental energy transport phenomena in nature, however, they have never been treated equally. The micro electronics, which is based on the inventions of electronic transistor and other relevant devices that control electric flow, has led to an impressive technological development that has changed many aspects of our life. Unfortunately, similar technology in direct controlling heat flow has still not been mastered by human being even though many-attempts have been made. Since in nature, original signals presented by heat are much more prevalent than those by electricity, the application of the latter one can be even more extensive. Thus one would like to know: *is "phononics", the counterpart of the electronics, that provides useful functions by controlling and managing heat current, only a dream?*

It is indeed much more difficult to artificially control the flow of heat in a solid, than to control the flow of electrons. The main reason is, unlike electrons, the carriers of heat -- *phonons* -- are not real particles with definite properties, but rather bundles of energy that have no mass and charge and are therefore unaffected by electromagnetic field. However, compared with the short, several-decade long history of our control over electronic flow, nature has been managing the flow of heat for billions of years, especially inside living bodies, just look at how exact the body temperature is controlled?

This fact not only raises an interesting question to us: how is it possible, but also provides us much confidence that it must be possible even if with completely different mechanism. Thanks to the rapid developments that have taken place in the recent years, we may finally be about to turn *phononics* from a dream into reality. In particular, researchers have recently built varies of heat flow control devices, e.g., thermal diodes and transistors etc, opening the door to functional thermal materials that control the flow of heat at the microscopic level. Moreover, by combining thermal transistors, all thermal logic gates and thermal memory are proposed which allow us to process information with phonons. Here we will demonstrate several basic phononic elements: thermal diode, thermal transistor, thermal logic gate and thermal memory.

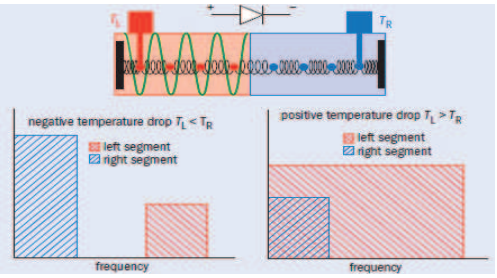

Figure 1. Thermal diode. By coupling two materials or "segments" with different resonant frequencies together, a thermal current can be stopped at or let through the interface depending on the temperatures of the segments (top). The right segment is an array of coupled nonlinear oscillators. The vibration frequency (red in bottom panel) depends on the vibrational amplitude – thus depends on the temperature. The right segment is an array of harmonic oscillator, thus its frequency does not change with temperature (blue in bottom panel). Therefore, in the case of $T_L > T_R$, there is current, whereas when $T_L < T_R$, there is no current. (Picture taken from Wang and Li [1])

Thermal diode: Thermal diode can rectify thermal current. In this device, when we apply temperature gradient in one direction, there is heat current flow through the system, however, when the temperature gradient is reversed the heat low is blocked. The physical principle of the diode is

Phononics 2011: First International Conference on Phononic Crystals, Metamaterials and Optomechanics
Santa Fe, New Mexico, USA, May 29-June 2, 2011
PHONONICS-2011-0042

illustrated in Fig 1. More details can be found in Ref.[1]. This basic phononic device has been demonstrated experimentally by using asymmetric nanotubes [2]

Thermal transistor: Like an electronic transistor, a thermal transistor consists of two segments, the source and the drain, as well as a third segment -the gate- through which the input signal is transferred (top). Crucially, negative differential thermal resistance (NDTR) is possible between the source and drain segments, which allows a heat current to be amplified. The transistor has two functions: switch and amplifier. The schematic picture is given in Fig. 2. More details can be found in Ref.[3]

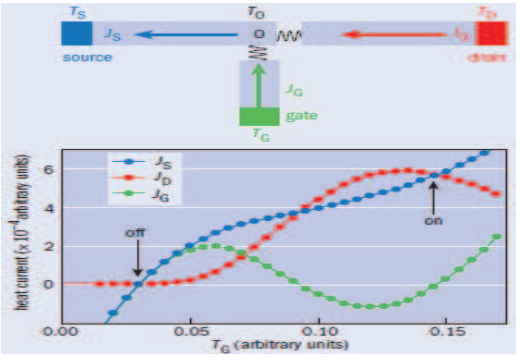

Figure 2: Thermal transistor

Calculations reveal that when the gate temperature (T_G) rises, both the drain current (J_D) and the source current (J_S) increase by a factor of almost 100. In particular, the gate current $J_G = J_S - J_D$ is zero when $T_G \approx 0.03$ and $T_G \approx 0.14$. Because the source current is so very different at the two temperatures, we can turn the transistor "off" by making $T_G = 0.03$ and switch it "on" by making $T_G = 0.14$. By making the thermal resistance between the output (O) and the gate very small, the temperature of the output (T_O) is always close to T_G. This switch function means that a thermal transistor can also be used to carry out thermal logic operations such as NOT, AND and OR. (Picture taken from Wang and Li [1].)

Thermal Logic gate: Thermal transistor provides not only the functions of thermal switch and thermal modulator which will greatly improve our ability to control heat flow, but also the essential functions of signal repeater and NOT gate: digitization and reversion. Based on the successful theoretical realization of thermal transistor, models of all thermal logic gates that can perform all logic operations have thus been presented recently [4]. We show the signal repeater (left panel), NOT gate (middle panel) and AND/OR Gate (right panel) in Figure 3. Details are given in [4].

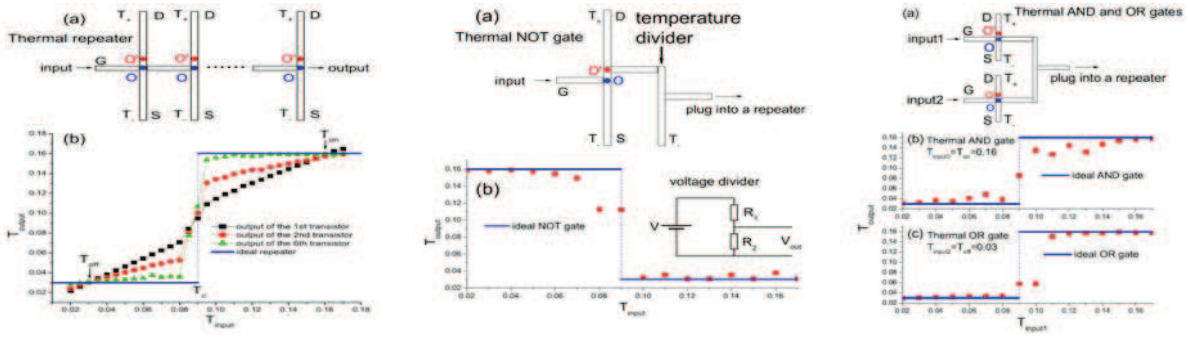

Figure 3. Thermal logic gates. Thermal **Repeater** (left panel), **NOT** gate (middle panel), **AND/OR** Gate (right panel)

Thermal Memory. Memory is an indispensable element for computer besides logic gates. Based on our thermal transistor model, we have demonstrated numerically the principle of thermal memory. Details can be found in Ref.[5]. Most recently, we have demonstrated it experimentally [6].

In summary, we have briefly shown phononic devices such as thermal diode, thermal transistor, thermal logic gate and thermal memory. Some of them have already been demonstrated experimentally. Phononics opens door for controlling and managing thermal current.

References

[1] B. Li, L Wang and G Casati, *Phys Rev. Lett* **93**, 184301 (2004); L Wang and B Li *Physics World* **21** (3), 27 (2008).
[2] C. W Chang, D. Okawa, A. Majumdar, and A. Zettl, *Science* **314**, 1121 (2006).
[3] B. Li, L Wang, and G Casati, *Appl. Phys. Lett.* **92**, 233504 (2006).
[4] L Wang and B Li, *Phys. Rev. Lett* **99,** 177208 (2007).
[5] L Wang and B Li, *Phys. Rev. Lett* **101**, 267203 (2008).
[6] R.-G Xie et al, *Adv. Funct Mat*. (2011) (in press).

Phononics 2011: First International Conference on Phononic Crystals, Metamaterials and Optomechanics
Santa Fe, New Mexico, USA, May 29-June 2, 2011
PHONONICS-2011-0046

Divide and Conquer Quantum Mechanical Methods for Phononic Applications

Rudolph C. Magyar[1]

[1] *Sandia National Laboratories, USA,*
rjmagya@sandia.gov

Abstract: Density functional theory is a highly efficient computational framework that describes structural properties of materials such as phonon frequencies and densities of states. In this talk, we suggest how the divide and conquer scheme may be well suited to determine phononic response in materials with supermolecular scale features.

Density functional theory is a highly efficient computational framework that describes structural properties of materials such as phonon frequencies and densities of states. Applications of DFT demonstrate the theory's reliability for calculating bond lengths and phonon frequencies. One of the greatest challenges to applying DFT to general problems is the increasing computational cost required when treating larger systems. Ideally, the cost would increase linearly with the number of atoms involved, but current workhorse implementations typically increase greater than quadratically. The divide and conquer scheme that was first proposed many years ago has seen a recent resurgence in the study of energetic materials and provides route towards linear scaling calculations of atomic forces and phonon frequencies. In this talk, we suggest how the divide and conquer scheme may be well suited to determine phononic response in materials with supermolecular scale features. We illustrate this with some examples using a computational tool newly developed at Sandia. Sandia National Laboratories is a multi-program laboratory operated by Sandia Corporation, a wholly owned subsidiary of the Lockheed Martin company, for the U.S. Department of Energy's National Nuclear Security Administration under contract DEAC04-94AL85000.

Phononics 2011: First International Conference on Phononic Crystals, Metamaterials and Optomechanics

Santa Fe, New Mexico, USA, May 29-June 2, 2011

PHONONICS-2011-0046

Phononics 2011: First International Conference on Phononic Crystals, Metamaterials and Optomechanics
Santa Fe, New Mexico, USA, May 29-June 2, 2011
PHONONICS-2011-0047

Predicting Phonon Properties Using the Spectral Energy Density

Alan J. H. McGaughey[1], Joseph E. Turney[1], John A. Thomas[1], Haibin Chen[1], Ryan M. Iutzi[1], Alexandre D. Massicotte[1], Cristina H. Amon[1,2]

[1] *Department of Mechanical Engineering, Carnegie Mellon University, Pittsburgh, PA, USA*
[2] *Department of Mechanical & Industrial Engineering, University of Toronto, Toronto ON, Canada*
mcgaughey@cmu.edu

Abstract: The spectral energy density technique for predicting phonon dispersion relations and relaxation times is presented. This technique, which uses atomic velocities obtained from a molecular dynamics simulation, incorporates the full anharmonicity of the atomic interactions. Results for a Lennard-Jones face centered cubic crystal are provided.

The usefulness of analytical models of thermal transport has been hampered by the necessary approximations and assumptions (e.g., a Debye solid, ignoring optical phonons), permitting only qualitative or semi-quantitative predictions.[1] When used with the Green-Kubo or direct methods, molecular dynamics (MD) simulations can predict thermal conductivity.[2-4] Because the analysis in these two methods is performed at the system level, however, no information about the phonons is obtained. The phonon properties needed to calculate thermal conductivity (group velocities, relaxation times) can be predicted using MD simulation and normal mode analysis, but this method requires *a priori* knowledge of the phonon frequencies and polarization vectors and is time-intensive.[2,5] Phonon frequencies and relaxation times can be obtained from harmonic and anharmonic lattice dynamics (LD) calculations, but these are theoretically and computationally complex and only valid at low temperatures.[5-8]

The spectral energy density (SED) presents a straightforward alternative by which phonon frequencies and relaxation times can be obtained using only atomic velocities from an MD simulation as input.[9-11] Here, we present the SED and describe how it can be used to obtain phonon frequencies and relaxation times, which can then be used to predict thermal conductivity. We calculate the SED using results from MD simulations of a test system of Lennard-Jones argon and compare the predicted phonon properties to predictions made using (i) anharmonic LD calculations and (ii) normal mode analysis performed on the results of the MD simulations.

The spectral energy density, Φ, is derived by projecting the velocities of the atoms in a crystal onto the normal modes of vibration. It is given by[11]

$$\Phi(\boldsymbol{\kappa},\omega)=\frac{1}{4\pi\tau_o N_T}\sum_\alpha\sum_b^B m_b\left|\int_0^{\tau_o}\sum_{n_{x,y,z}}^{N_T} v_\alpha\left(n_{x,y,z},b;t\right)\,\exp\left[i\boldsymbol{\kappa}\cdot\mathbf{r}\left(n_{x,y,z},0\right)-i\omega t\right]dt\right|^2, \quad (1)$$

where $v_\alpha(n_{x,y,z},b;t)$ is the α-direction velocity of atom b (with mass m_b) in unit cell $n_{x,y,z}$, $\mathbf{r}(n_{x,y,z},0)$ is the equilibrium position of unit cell $n_{x,y,z}$, B is the number of atoms in the unit cell, N_T is the total number of unit cells, t is time, τ_o is the length of the simulation, $\boldsymbol{\kappa}$ is wave vector, and ω is frequency.

The frequency dependence of the SED for a face-centered cubic Lennard-Jones argon crystal at a temperature of 20 K at selected wave vectors along the [100] direction is shown in Figs. 1(b), 1(c), and 1(d). There is a clear correlation between the locations of the frequency peaks and frequencies calculated using harmonic lattice dynamics calculations, which are shown in the [100] dispersion curves plotted in Fig. 1(a). For each phonon mode, the range of frequencies accessed by the atoms is related to the anharmonicity of the interatomic potential and the corresponding rate of multi-phonon scattering processes. For fixed wave vector, the frequency spread is the Lorentzian function[11]

$$\Phi(\boldsymbol{\kappa},\omega)=\frac{I}{1+[2\tau(\omega-\omega_c)]^2}, \quad (2)$$

Phononics 2011: First International Conference on Phononic Crystals, Metamaterials and Optomechanics
Santa Fe, New Mexico, USA, May 29-June 2, 2011
PHONONICS-2011-0047

where I is the peak height, ω_c is the peak location (i.e., the phonon frequency), and τ is the relaxation time. Thus, by fitting Eq. (2) to each peak in the SED, it is possible to obtain the phonon frequencies and relaxation times. The frequencies plotted versus wave vector give the phonon dispersion curves. The phonon group velocity is the slope of the dispersion curve.

A selection of the relaxation times extracted from the SED plots shown in Fig. 1 are provided in Table 1. The table also includes predictions made using the normal-mode decomposition MD method and anharmonic LD calculations. The normal-mode decomposition predictions are made using the same simulations as those used for the SED. The agreement between the SED method and the normal-mode decomposition method is generally good, as in both methods, the system energy is being mapped from direct space and time to reciprocal space and frequency. The agreement with the anharmonic LD predictions is not as good. This result may be due to the low temperature approximations inherent in LD techniques. The normal-mode decomposition method will lose accuracy at higher temperatures because quasi-harmonic phonon frequencies and polarization vectors are used to perform the energy mapping. The SED method, however, does not suffer from this limitation and should be applicable at higher temperatures as long as the weakly-interacting phonon interpretation is valid.

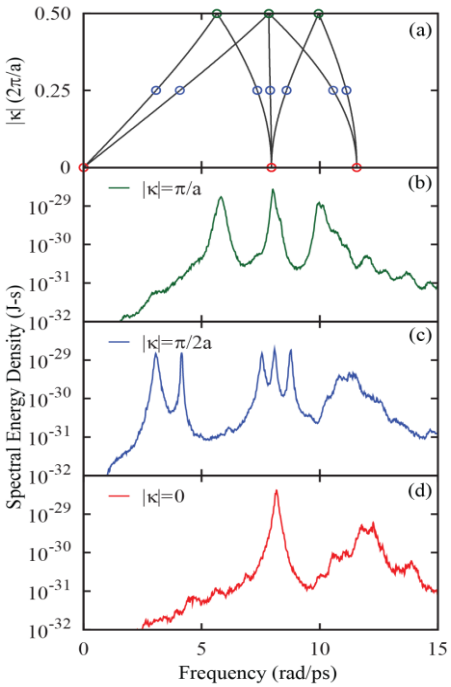

Figure 1 (a) LJ argon [100] dispersion based on a four-atom conventional unit cell representation. (b), (c) and (d): Spectral energy density at select points in the [100] direction at a temperature of 20 K. The modes indicated with open circles on the dispersion curves can be seen as peaks in the SED.

$\|\kappa\|$	Frequency (1/ps)	Spectral Energy Density	Normal Mode Decomposition	Anharmonic Lattice Dynamics
0	8.17	6.02	5.15	12.7
0	12.0	1.10	1.36	1.45
π/a	3.07	5.45	7.43	6.74
π/a	11.4	1.19	1.29	1.57
$2\pi/a$	5.81	3.32	4.28	6.68
$2\pi/a$	10.0	2.47	2.58	4.19

Table 1 Lennard Jones argon [100] relaxation times at 20 K in ps predicted by three different methods.

References

[1]M. G. Holland, *Phys. Rev.* **132**, 2461-2471 (1963).
[2]A. J. H. McGaughey and M. Kaviany, *Phys. Rev. B* **69**, 094303 (2004).
[3]P. K. Schelling, S. R. Phillpot, and P. Keblinski, *Phys. Rev. B* **65**, 144306 (2002).
[4]D. P. Sellan, E. S. Landry, J. E. Turney, A. J. H. McGaughey, and C. H. Amon, *Phys. Rev. B* **81**, 214305 (2010)
[5]A. J. C. Ladd, B. Moran, and W. G. Hoover, *Phys. Rev. B* **34**, 5058-5064 (1986).
[6]A. A. Maradudin and A. E. Fein, *Phys. Rev.* **128**, 2589-2608 (1962).
[7]D. C. Wallace, *Thermodynamics of Crystals*, Cambridge University Press, UK (1972).
[8]J. E. Turney, E. S. Landry, A. J. H. McGaughey, and C. H. Amon, *Phys. Rev. B* **79**, 064301 (2009).
[9]S. Maruyama, *Nano. Micro. Therm. Eng.* **7**, 41-50 (2003).
[10]N. de Koker, *Phys. Rev. Lett.* **103**, 125902 (2009).
[11]J. A. Thomas, J. E. Turney, R. M. Iutzi, C. H. Amon, and A. J. H. McGaughey, *Phys. Rev. B* **81**, 081411(R) (2010).

Phononics 2011: First International Conference on Phononic Crystals, Metamaterials and Optomechanics

Santa Fe, New Mexico, USA, May 29-June 2, 2011

PHONONICS-2011-0049

Heat dissipation in silicon and quartz nanoridges

Pierre-Olivier Chapuis[1,a,*], Mika Prunnila[2], Andrey Shchepetov[2,a], Lars Schneider[1], Emigdio Chavez[1,3], Sampo Laakso[2], Jouni Ahopelto[2], and Clivia M. Sotomayor Torres [1,3,4]

[1] Institut Català de Nanotecnologia (ICN), Centre d'Investigacio en Nanociencia e Nanotecnologia (CIN2), Campus UAB, 08193 Bellaterra (Barcelona), Spain

[2] VTT Microelectronics, PO Box 1000, 02044 VTT, Espoo, Finland

[3] Department of physics, Universitat Autonoma de Barcelona, 08193 Bellaterra (Barcelona), Spain

[4] Institució Catalana de Recerca i Estudis Avançats (ICREA), 08010 Barcelona, Spain

[1] These authors contributed equally.

[*] E-mail: olivier.chapuis@cin2.es

Abstract: We have investigated experimentally the effect of confinement of thermal acoustic phonons in 100 nm large ridges of silicon and quartz. We quantify the deviation to Fourier and ballistic predictions as a function of two characteristic numbers, the constriction Knudsen number describing the transmission of the phonons and a dimensionless number based on the nanoridges volume/surface ratio.

We have investigated experimentally the effect of lateral confinement of thermal acoustic phonons in nanoridges of silicon and of quartz as a function of the temperature. Electrical methods are used to generate phonons in 100nm large nanostructures and to probe the nanostructure temperature in the same time, what allows tracking the heat flux generated and its possible deviation to Fourier diffusive heat conduction. It is now well-established that Fourier's law of heat diffusion in solids breaks down when device sizes reaches the nanometer-scale[1]. Detailed studies of the characteristic lengths where the law has to be replaced or modified are required as these lengths might depend on the considered device geometries. We have fabricated special devices made of nanostructured ridges on top of planar substrate as represented on Figure 1. The top of a ridge is a wire made either of metal or of doped silicon that acts as a heater and as a thermometer in the same time. The lower part that supports the wire is made of an etched part of the wafer substrate of silicon or quartz. This type of structure enables to generate phonons in the ridge and to measure the heat flux flowing to the substrate.

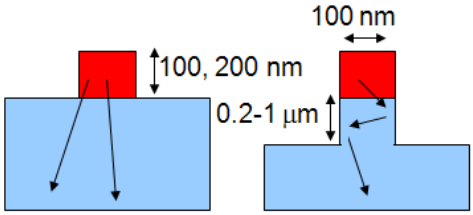

Figure 1 *Schematic of the nanostructures*

Different electrical methods such as the 3ω method[2] are used to heat the wire. The goal is then to measure a wire-voltage component (dc or ac) proportional to the wire temperature. A model enables then to link the wire temperature to the heat flux transmitted to the substrate. In addition to the localized heat source effect due to the sub-mean free path size of the source[3], we have investigated experimentally the consequences of the fact that the source cannot be considered as a proper heat bath at equilibrium.

Phononics 2011: First International Conference on Phononic Crystals, Metamaterials and Optomechanics

Santa Fe, New Mexico, USA, May 29-June 2, 2011

PHONONICS-2011-0049

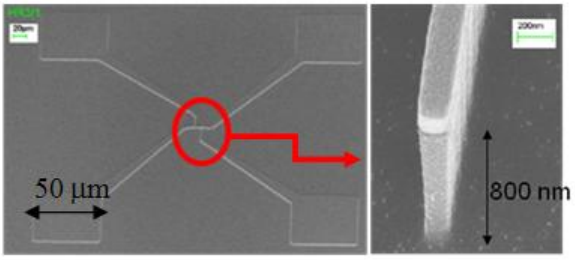

Figure 2 *Electrical accesses and ridge before mask removal*

We have quantified the effect as a function of the two characteristic numbers that can be associated with the problem, namely the constriction Knudsen number describing the transmission of the phonons and the nano-structure Knudsen number characterizing the nonequilibrium of the source. We compare our results with those of a recent theoretical paper[4] based on the ballistic-diffusive equations. The determination of the mean free paths of phonons as a function of the frequency remains a key point due to the consequences for heat transport and thermal management[1].

We observe a strong decrease of the thermal conductance through the ridge in comparison to a prediction based on the Fourier diffusive as expected. But, more strikingly, we also observe a decrease in comparison to the ballistic prediction. We aim at ascribing part of this decrease to an effect of phonon confinement in the ridge.

Acknowledgements

We acknowledge the support of EU FP7 projects NANOPACK and NANOPOWER. We also acknowledge the support of Spanish MICINN project ACPHIN.

References

[1] D. G. Cahill, W. K. Ford, K. E. Goodson, G. D. Mahan, A. Majumdar, H. J. Maris, R. Merlin, S. R. Phillpot, J. Applied Physics 93, 793-818 (2003).
[2] D. Cahill, Rev. Scient. Instr. 61, 802 (1990)
[3] M.E. Siemens, Q. Li, R. Yang, K.A. Nelson, E.H. Anderson, M.M. Murnane, and H.C. Kapteyn, Nature Materials 9, 26 (2010)
[4] S. Volz and P.O. Chapuis, J. Applied Physics 103, 34306 (2008)

Phononics 2011: First International Conference on Phononic Crystals, Metamaterials and Optomechanics
Santa Fe, New Mexico, USA, May 29-June 2, 2011
PHONONICS-2011-0050

Temperature and Size Dependence of Thermal Conductivity in Single Crystal ZnO Nanowires

Cong-Tinh Bui[1], Rongguo Xie[2], Baowen Li[1, 2, 3], John T. L. Thong[1, 4]

[1] *NUS Graduate School for Integrative Sciences and Engineering, National University of Singapore, Singapore 117456, Republic of Singapore, tinhbc@nus.edu.sg*
[2] *Department of Physics, National University of Singapore, Singapore 117542, Republic of Singapore, xierg2001@nus.edu.sg*
[3] *Centre for Computational Science and Engineering (CCSE), National University of Singapore, Singapore 117456, Republic of Singapore, phylibw@nus.edu.sg*
[4] *Department of Electrical and Computer Engineering, National University of Singapore, Singapore 117576, Republic of Singapore, john_thong@nus.edu.sg*

Abstract: We report on measurements of thermal conductivity (κ) of single crystal zinc oxide (ZnO) nanowires. The thermal conductivity firstly increases and then decreases with temperature as $T^{-\alpha}$ (α in the range of 1.42 – 1.49). Thermal conductivity is also found to be increased linearly with the cross-section area (~d^2) of nanowires in studied diameter range.

Introduction

Zinc oxide (ZnO) is a wide and direct band gap (3.5 eV at room temperature) oxide semiconductor. It has attracted a lot of research interest because of its optoelectronic and electronic properties[1, 2]. ZnO nanowires owning unique physical properties have been demonstrated to be promising for various applications such as piezoelectronic power generators, field effect transistors, piezoelectric sensors, etc. Since most applications are related to high-power electronic and optoelectronic device, it is necessary to understand the thermal behaviour of ZnO nanowires. In this work, we have studied temperature and size dependence of thermal conductivity of single crystal ZnO nanowires in order to understand phonon transport mechanism behind thermal behaviour in 1-dimensional lattice structures.

Measurement method

Single crystal ZnO nanowires used in this study were synthesized via vapor transport process in a sealed horizontal tube. The micro-thermal measurement (MTM) devices was fabricated and measurement method was described similarly with those of others previously[3, 4]. MTM devices consist of two suspended SiN_x membranes with Pt loops. One membrane serves as a heater to create temperature gradient and the other serves as a sensor to measure the temperature change. A nano-manipulator in SEM chamber was then used to pick up and place single ZnO nanowire onto the MTM device. The Pt/C composite pads were then deposited on two ends of nanowires using focus electron beam to reduce thermal contact resistance as well as to stick nanowires to the membranes. Fig. 1 shows scanning electron microscope (SEM) image of the MTM device with single ZnO nanowire. In this study, we have prepared and measured thermal conductivity of five ZnO nanowire samples with diameter of 70; 84; 120; 166; and 209 nm. For each sample, the measurement was performed in vacuum chamber with temperature varies from 77K to 400K which is controlled by cryostat.

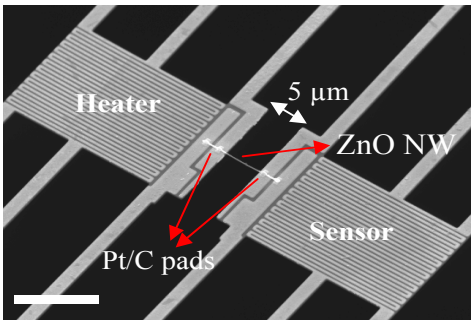

Figure 1 SEM image of ZnO nanowire sample on micro-thermal measurement device. Scale bar: 10μm

Results and Discussion

Fig.2 shows the measured thermal conductivity (κ) as a function of temperature for ZnO nanowires. For all samples, when the temperature increases κ increases to maximum value (at turnover temperature between 120 and 150K) and then decreases. κ at room temperature for 70; 84; 120; 166; and 209 nm diameter nanowires is 7.04; 7.52; 9.06 11.78 and 14.41 W/m.K, respectively, which is one order of magnitude lower than that of bulk ZnO. To understand thermal transport in ZnO nanowires, we

Phononics 2011: First International Conference on Phononic Crystals, Metamaterials and Optomechanics
Santa Fe, New Mexico, USA, May 29-June 2, 2011
PHONONICS-2011-0050

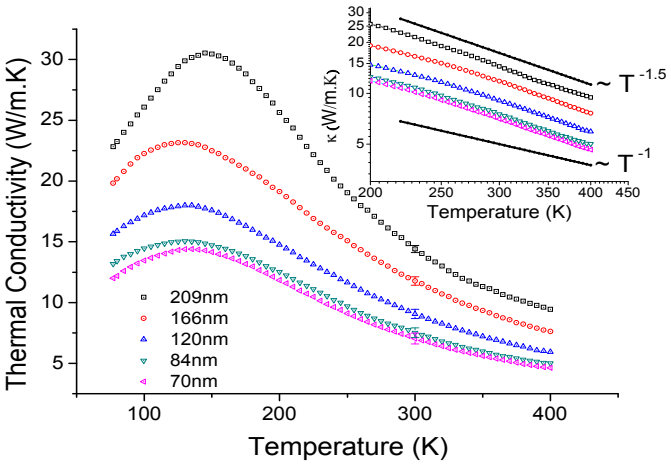

Figure 2 Temperature dependence of thermal conductivity of ZnO nanowires with different diameters. Inset: log-log scale in temperature range 200K – 400K.

consider all phonon scattering processes which induce thermal resistance in single crystal nanowires. The phonon relaxation time corresponding to various scattering mechanisms is employed to describe thermal transport. The total inverse phonon relaxation time, which is followed Matheissen's rule, equals to the sum of the inverse relaxation time corresponding to boundary scattering, phonon – phonon scattering (including normal three-phonon processes and Umklapp processes), and impurity/isotope scattering[5]

$$\tau^{-1} = \tau_b^{-1} + \tau_p^{-1} + \tau_i^{-1} \quad (1)$$

The behaviour of the observed thermal conductivity with temperature can be explained qualitatively as follows: at low temperature phonon mean free path is larger. Phonon will be scattered with the boundary before colliding with other phonons. The boundary scattering predominates and the thermal conductivity increases with temperature. When the temperature increases, it is easier to create higher frequency phonons which are scattered efficiently by impurities, hence the isotope scattering rapidly becomes dominant. Consequently, the thermal conductivity reaches a maximum and then declines. As the temperature further increases, normal three-phonon scattering and umklapp scattering become important and dominate over the isotope scattering. As the result, thermal conductivity of nanowires further decreases with increasing temperature. The temperature dependence of thermal conductivity of ZnO nanowires between 200 and 400K is plotted logarithmically in the inset of Fig.2. We observed that, after the maximum at low temperature, thermal conductivity decreases following the power law $T^{-\alpha}$. For all five ZnO nanowires, the measurement results give a factor α in the range of 1.42 to 1.49 which is close to that of Callaway's model for lattice thermal conductivity taking into account the boundary scattering[6] (α = 1.5).

The size dependence of thermal conductivity of ZnO nanowires were show in Fig. 3, in which κ is plotted as function of d^2. In the measured diameter range, thermal conductivity increases with increasing of cross-section area. This effect is obviously understood because of less phonon boundary scattering for larger nanowires and hence will reach to saturation when diameter of nanowire goes to certain value (bulk limit). Interestingly, κ increases almost linearly with cross-section area in studied diameter range, especially at room temperature (300K).

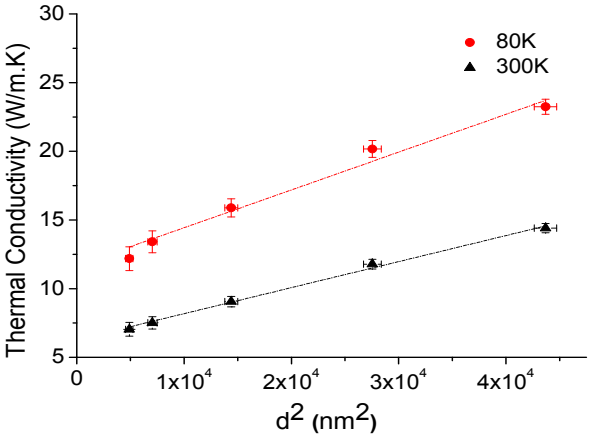

Figure 3 Diameter dependence of thermal conductivity of ZnO nanowires at 80K and 300K. Dash-dot lines are to guide eyes.

References

[1] Z. K. Tang, G. K. L. Wong, and P. Yu, *Appl. Phys. Lett.* **72**, 3270-3272 (1998).
[2] A. Tsukazaki, A. Ohtomo, T. Onuma, M. Ohtani, T. Makino, M. Sumiya, K. Ohtani, S. F. Chichibu, S. Fuke, Y. Segawa, H. Ohno, H. Koinuma, and M. Kawasaki, *Nat. Mater.* **4**, 42-46 (2005).
[3] L. Shi, D. Li, C. Yu, W. Jang, D. Kim, Z. Yao, P. Kim, and A. Majumdar, *J. Heat Transf.* **125**, 881-888 (2003).
[4] Z. Wang, R. Xie, C. T. Bui, D. Liu, X. Ni, B. Li, and J. T. L. Thong, *Nano Lett.*, Article ASAP (2010).
[5] M. A.Palmer, K. Bartkowski, E. Gmelin, M. Cardona, A. P. Zhenov, A. V. Inyushkin, A. Taldenkov, V. I. Ozhogin, K. M. Itoh, and E. E. Haller, *Phys. Rev. B* **56**, 9431-9447 (1997).
[6] J. Calaway, *Phys. Rev.* **113**, 1046-1051 (1959).

Phononics 2011: First International Conference on Phononic Crystals, Metamaterials and Optomechanics
Santa Fe, New Mexico, USA, May 29-June 2, 2011
PHONONICS-2011-0051

Phononic Thermal Transport in Thin Nanoscale Membranes

Ilari J. Maasilta[1], Jenni T. Karvonen[1], Thomas Kühn[1]

[1] *Nanoscience Center,Department of Physics, P. O. Box 35, FI-40014 University of Jyväskylä, Finland*
maasilta@jyu.fi

Abstract: We have studied experimentally the thermal conductance of thin free-standing silicon nitride membranes at sub-Kelvin temperatures as a function of membrane thickness between 40 nm and 750 nm, using normal metal-insulator-superconductor (NIS) thermometry. Effects of dimensionality cross-over from 3D to 2D phonons are seen, however not all observations follow the simplest theory.

Introduction

It is essential to understand the thermal transport properties of thin insulating membranes from the point of view of applications. Often devices, such as bolometric low-temperature radiation detectors[1], are placed on top free standing silicon nitride membranes (SiN) so that the thermal isolation from the environment can be engineered. Although heavily used in applications, the fundamental understanding of the physics of phonon transport in thin membranes is still not deeply understood, however. Only a few previous experiments have been performed at sub-Kelvin temperature range [2-4], with very little emphasis on the interpretation of the results.

On the other hand, theoretical advances in recent years have discussed some interesting results, especially in the limit where the membrane becomes so thin that only the lowest two-dimensional (2D) phonon modes are occupied at low temperatures[5-7]. In this case, the usual 3D plane wave phonon modes are not eigenmodes anymore: instead more complex displacement field distributions occur in the direction perpendicular to the membrane plane. These phonon modes (Lamb-modes) have been known in acoustics since the work of Rayleigh and Lamb in late 1800's. However, only recently has their importance in low-temperature thermal transport been investigated further [5-7]. Theoretical results predict that for the Lamb-modes, the temperature dependence of thermal conductance G should change from the 3D case, from the usual $G \sim T^3$ to a weaker $G \sim T^{1.5}$ at the lowest temperatures, if the phonon transport is ballistic [6] or if it is diffusive but limited by a constant (non temperature dependent) mean free path [5]. Even more interestingly, at a constant temperature, the thermal conductance depends inversely on the membrane thickness d as $G \sim 1/\sqrt{d}$: in other words, thinner membranes have higher thermal conductance [6,7].

The experiment

Here, we present the first experiments on phonon thermal transport in thin silicon nitride (SiN) membranes that clearly span the expected 3D-2D crossover for SiN: The theoretical crossover temperature is given[6,7] by $T_{cr} = \hbar c_t/(2k_B d)$, where c_t is the transverse speed of sound. This predicts $T_{cr} \sim 0.6$ K for the thinnest membranes in this study with d= 40 nm, and means that our experiment, reaching a temperature of 0.1 K, is well within the 2D limit. Two other membrane thicknesses were studied for comparison: d= 200 nm and d= 750 nm. Both of these samples are expected to be in the 3D limit. Our recent experiments on electron-phonon interaction in metal wires fabricated on similar suspended SiN membranes have in fact confirmed that the thinnest membrane is in the 2D limit[8].

The membranes were fabricated using standard bulk micromachining techniques[8] by chemically etching the Si substrate in KOH. A circular shaped Cu wire heater (radius 7 μm, width ~ 300 nm, thickness 30 nm) was fabricated at the center of the membrane, which was typically of a size 500 μm x 500 μm. The Cu heater was connected by superconducting Nb leads to the external voltage source used for heating. This ensured that all the Joule heat was dissipated in the Cu wire. A superconductor-insulator-normal metal-insulator-superconductor (SINIS) tunnel junction pair was placed some specified distance away from the heater, and used for thermometry. More details on the sample fabrication and SINIS thermometry can be found in Refs. 9,10.

Phononics 2011: First International Conference on Phononic Crystals, Metamaterials and Optomechanics
Santa Fe, New Mexico, USA, May 29-June 2, 2011
PHONONICS-2011-0051

By sweeping the heater voltage and measuring the current and voltage across the wire, one can measure the dissipated phonon power P emitted from the heater, in addition to the temperature T at the SINIS thermometer, and study how the temperature rises with given power input. Differential thermal conductance could then be computed as $G = \partial P/\partial T$. Representative results for P vs. T curves for all membrane thicknesses are shown in Fig. 1 for a thermometer that was located ~40 μm away from the center of the heater.

The first main conclusion from the data is: The temperature exponent is a bit surprisingly approximately the same for all membrane thicknesses. In terms of G, the observed dependence is $G \sim T^{2.5}$ ($P \sim T^{3.5}$). This does not agree with the simplest theories either for 3D or for the 2D limit. The only possible explanation is that some scattering mechanism for phonons exists in the membranes with a temperature dependent mean free path. One likely mechanism could be two-level systems[11], as the membranes are amorphous and are known contain lots of them.

On the other hand, the absolute values of the conductance do change with thickness. For 3D phonon transport, the emitted power at a given T should simply scale linearly with d. Looking at Fig.1 this is clearly not the case: in fact the 40 nm membrane power is higher than the 200 nm one at temperatures below 0.4 K. This observation qualitatively agrees with the theoretical results on thickness dependence of the Lamb modes in the 2D limit[6,7].

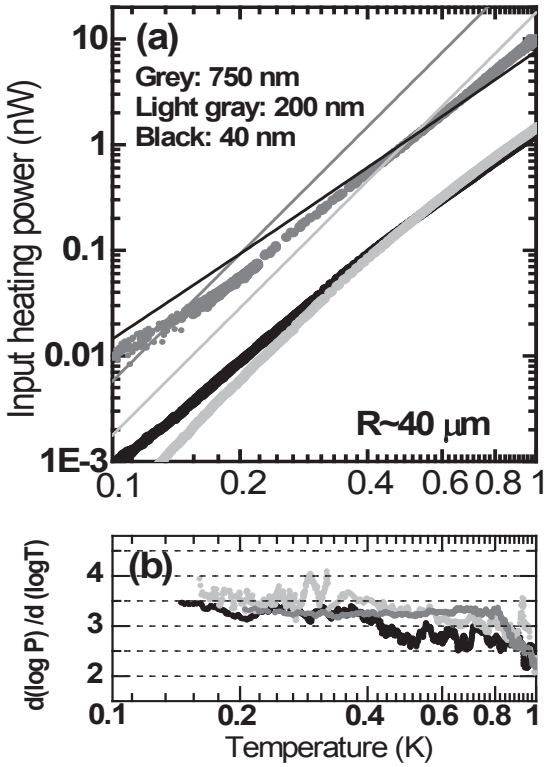

Figure 1 (a) Measured input heating power vs. phonon temperature. SINIS thermometer was 40 μm away from the center of the heater. Lines show the expected theoretical curves in the ballistic limit for each membrane thickness. (b) The logarithmic derivative of the data, giving the temperature exponent.

Lastly, we have plotted the theoretical upper limits for the power vs. temperature in Fig. 1 based on the ballistic limit theory (3D theory for 750 and 200 nm, 2D theory for 40 nm). It is clear that the 750 nm membrane is essentially at the ballistic limit at 0.1 K, in agreement with earlier data[2]. However, the thinner membranes start to deviate more and more, with the 40 nm results being furthest from the ballistic limit. More detailed modeling including diffusive surface scattering is in progress to understand the experiments more deeply.

References

[1] Ch. Enss, ed., *Cryogenic Particle Detection*, Springer, Heidelberg (2005).
[2] W. Holmes, J. M. Gildemeister, P. L. Richards, and V. Kotsubo, *Appl. Phys. Lett.* **38**, 2250 (1998).
[3] M. M. Leivo and J. P. Pekola, *Appl. Phys. Lett.* **70**, 1305 (1998).
[4] H. F. C. Hoevers, M. L. Ridder, A. Germeau, M. P. Bruijn, and P. A. J. Korte, *Appl. Phys. Lett.* **86**, 251903 (2005).
[5] T. Kühn, D. Anghel, J. Pekola, M. Manninen, and Y. Galperin, *Phys. Rev. B.* **70**, 125425 (2004).
[6] T. Kühn and I. J. Maasilta, *Nucl. Instr. and Meth. A* **559**, 724 (2006).
[7] T. Kühn and I. J. Maasilta, *J. Phys. Conf. Series* **92**, 012082 (2007).
[8] J.T. Karvonen and I.J. Maasilta, *Phys. Rev. Lett.* **99**, 145503 (2007).
[9] P.J. Koppinen and I.J. Maasilta, *Phys. Rev. Lett.* **102**,165502 (2009).
[10] J. T. Karvonen, Ph. D. Thesis, University of Jyväskylä (2009).
[11] T. Kühn, D. V. Anghel, Y. M. Galperin, and M. Manninen, *Phys. Rev. B* **76**, 165425 (2007).

Phononics 2011: First International Conference on Phononic Crystals, Metamaterials and Optomechanics
Santa Fe, New Mexico, USA, May 29-June 2, 2011
PHONONICS-2011-0078

Coherent phonons in polycrystalline bismuth film monitored by ultrafast electron diffraction

A. Bugayev and H. E. Elsayed-Ali

Applied Research Center, Old Dominion University, Norfolk, VA 23529,USA,

abugayev@odu.edu, helsayed@odu.edu

Abstract: The generation of coherent phonons in polycrystalline bismuth film is observed by ultrafast time-resolved electron diffraction. The dynamics of the diffracted intensities from the (110), (202), and (024) lattice planes show pronounced oscillations at 130–150 GHz. The anisotropy in the energy transfer rate of coherent optical phonons is discussed.

The interaction of femtosecond laser pulses with semimetals and semiconductors produces electronic excitations coupled with lattice vibrations through the deformation potential and stimulated Raman scattering . If the frequencies of Raman active phonons in the laser-excited material are smaller than the inverse duration of the laser pulse, then the laser-induced change in the equilibrium positions of the nuclei (displacive excitation) results in generation of coherent optical and acoustical phonons. Numerous studies were performed on the dynamics of coherent phonons in bismuth (Bi) by monitoring of the optical reflectivity modulation with femtosecond pump-probe techniques, and by femtosecond time-resolved X-ray diffraction of lattice dynamics [1-4].

We report on the characteristics of coherent phonons as observed in modulation of temporal behavior of the electron-diffracted intensities from three (110), (202), and (024) lattice planes of polycrystalline free-standing 22±2 nm thick Bi film. An electron gun, described in our previous publication [5], was used to produce electron pulses of ~1.5 ps duration by photoemission from silver thin film photocathode excited by frequency-tripled femtosecond (110 fs duration, 800 nm wavelength, at 1 kHz repetition rate) laser pulses. The Bi film was exposed to the fundamental 800 nm wavelength at a pulse energy density ~2 mJ/cm^2 that corresponds to excited carrier's density ~10^{21} cm^{-3}. The intensity changes of the diffraction rings are given in terms of contrast value $V(r) = (I(r) - I_{bg}(r))/(I(r) + I_{bg}(r))$ ($I_{bg}(r)$ is the background intensity distribution), which takes into account both the changes in diffraction peak and background intensities after the laser exposure. Each time-resolved electron diffraction scan was acquired twice and the average value was used for analysis. To analyze the data, the Boltzmann (sigmoidal) fit was used such that $V(\tau) = V_{min} + (V_{max} - V_{min})/(1 + \exp(\frac{\tau - \tau_{infl}}{\tau_{rate}}))$ where τ_{infl} is the inflection point of the dependence of $V(\tau)$ on the delay time τ, and τ_{rate} is the rate (slope) of the process at this point. The dynamics of the intensity change $V(\tau)$ were characterized by the coordinate of the inflection point τ_{infl} and by the drop-off intensity time τ_{hkl}, which is determined as the full width at e^{-1} level of the maximum of the first derivative of the Boltzmann fit. The Fourier transform was used for frequency analysis.

The temporal development of the contrast values $V(r)$ of the diffraction orders as a function of delay time is shown in Figure. It is seen that all three diffraction orders $I_{hkl}(\tau)$ follow the same temporal behavior, namely, the intensity decrease, which is accompanied with high frequency oscillations in a frequency band centered at 130–150 GHz (see insets in Figure). Since an optical phonon can emit two acoustic phonons, different combinations of two or more phonons can give rise to a generation of new phonon frequencies like $A_{1g}(\Gamma) \rightarrow 2\mathrm{LA}(\Lambda)$, $A_{1g}(\Gamma) \rightarrow \mathrm{LA}(T) + \mathrm{LA}(X)$, $2\mathrm{LA}(X) - \mathrm{LA}(\Lambda) \rightarrow \mathrm{TA}(X)$, and so on. Therefore, one can find that the combination $A_{1g}(\Gamma) - E_g(\Gamma) - 2\mathrm{LA}(X)$ yields the phonon frequency 134 GHz, which is in good agreement with our results. An interesting feature is the different drop time in the diffraction orders τ_{hkl} extracted from the Boltzmann fit, which are τ_{110} ~ 8.6 ps, τ_{202} ~ 18 ps, and τ_{024} ~ 7.8 ps. In general, two mechanisms could contribute to the energy transfer $\tau_{e\text{-}ph}$ from electrons to the phonon subsystem resulting in lattice heating. The first one is direct-energy transfer from electrons to phonons through optical phonon decay. This can be evaluated from the following $\tau_{e-ph} \approx (\hbar\omega_D^2 T_L^2 / T_D^2 \varepsilon_F)$ ratio (here ω_D, T_D, T_L is the Debye frequency, the Debye temperature, and lattice temperature, respectively, ε_F is the Fermi level). At our experimental conditions, the energy transfer rate $\tau_{e\text{-}ph}$ is 5–20 ps. The second mechanism affecting $\tau_{e\text{-}ph}$ is the electron-hole pair recombination

Phononics 2011: First International Conference on Phononic Crystals, Metamaterials and Optomechanics
Santa Fe, New Mexico, USA, May 29-June 2, 2011
PHONONICS-2011-0078

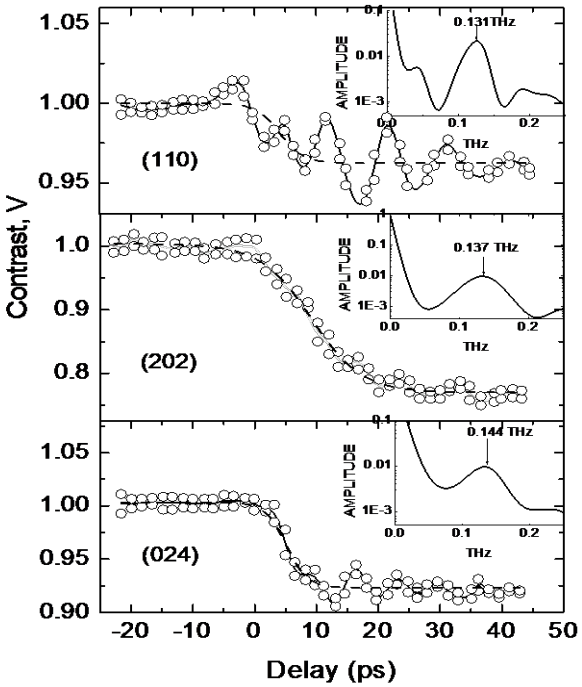

Figure 1 Normalized contrast $V(r)$ of diffraction orders as a function of the delay time. Dashed line is Boltzmann fit. Solid line is to guide the eyes only. Insets show the the Fourier transform.

accompanied by phonon emission. For Bi at room temperature this process can be as fast as a 2–3 ps [6].

The energy transfer depends on the lattice plane {*hkl*} of Bi. The anisotropy manifests itself not only in different drop time τ_{hkl} but also in different time of the inflection points: the maximum slope of the intensity change is achieved at ~ 5 ps for (110), at ~ 9 ps for (202), and at ~ 4 ps for (024) lattice planes. Hence, the drop-off amplitude of the intensity of the diffraction orders does not follow a single Debye-Waller factor written for the harmonic approximation as $V_g = V_g^0 \exp(-Bs^2) = V_g^0 exp\left[-B(T)\left(\frac{\sin\theta}{\lambda}\right)^2\right]$ (here V_g^0 denotes the structure factor of a perfect crystal, θ is the Bragg scattering angle, λ is the electron wavelength, and $B(T)$ is the Debye-Waller factor). According to this expression, the decrease in the intensity of the diffracted beam is expected to be more pronounced for high-order diffraction, but this is not supported by our measurements shown in Figure 1. Two mechanisms can possibly affect the expected dynamics of the intensity decay. The first one is the anisotropy of $B(T)$ for bismuth caused by the different means-square displacements of the atoms parallel $B_\parallel(T)$ and perpendicular $B_\perp(T)$ to the hexagonal *c* axis [7]. For Bi, $B_\perp(T) = 2B_\parallel(T)$ at $T = 293$ K and $B_\perp(T) = 8B_\parallel(T)$ at $T = 516$ K, therefore, the influence of anisotropy is very considerable. The second mechanism is the atomic motion of coherent optical phonons A_{1g} that takes place along the elongated body diagonal, whereas the atomic motion of E_g phonons occurs in the plane perpendicular to this diagonal [8]. The combined action of these two mechanisms on the differently oriented planes (110), (202), and (024) can result in significant change of the energy transfer rate of coherent optical phonons as well as of the amplitude of the diffraction intensity response.

This work was supported by Department of Energy and National Science Foundation. We acknowledge the contribution of A. Esmail and M. Abdel-Fattah in construction of the diffraction system.

References

[1] A. Q. Wu and X. Hu, "Coupling of ultrafast laser energy to coherent phonons in bismuth", Appl. Phys. Lett. 90, 251111/1-251111/3 (2007)
[2] M. F. DeCamp, D. A. Reis, P. H. Bucksbaum, and R. Merlin, "Dynamics and coherent control of high-amplitude optical phonons in bismuth", Phys. Rev B 64, 092301/1-092301/3 (2001).
[3] D. Boschetto, E. G. Gamaly, A. V. Rode, B. Luther-Davies, D. Glijer, T. Garl, O. Albert, A. Rousse, and J. Etchepare, "Small Atomic Displacements Recorded in Bismuth by the Optical Reflectivity of Femtosecond Laser-Pulse Excitations" Phys. Rev. Lett. **100**, 027404/1-027404/4 (2008).
[4] K. Sokolowski-Tinten, C. Blome, J. Blums, A. Cavalleri, C. Dietrich, A. Tarasevitch, I. Uschmann, E. Förster, M. Kammler, M. Horn-von-Hoegen, and D. von der Linde, "Femtosecond X-ray measurement of coherent lattice vibrations near the Lindeman stability limit", Nature, **422**, 287-289 (2003).
[5] B.-L. Qian and H. E. Elsayed-Ali, "Electron pulse broadening due to space charge effects in a photoelectron gun for electron diffraction and streak camera systems", J. Appl. Phys. **91**, 462-469 (2002).
[6] A. A. Lopez, "Electron-hole rcombination in bismuth", Phys. Rev. **175**, 823-840 (1968).
[7] P. Fisher, I. Sosnowska, and M. Szymanski, "Debye-Waller factor and thermal expansion of arsenic, antimony and bismuth", J. Phys. C: Solid State Phys. **11**, 1043-1051 (1978).
[8] E. S. Zijlstra, L. L. Tatarinova, and M. E. Garcia, "Laser-induced phonon-phonon interactions in bismuth", Phys. Rev. B74, 220301/1-220301/4 (2006)

Phononics 2011: First International Conference on Phononic Crystals, Metamaterials and Optomechanics
Santa Fe, New Mexico, USA, May 29-June 2, 2011
PHONONICS-2011-0080

Phonon scattering at structurally variant boundaries

Patrick E. Hopkins

[1] *Engineering Sciences Center, Sandia National Laboratories, 1515 Eubank SE, Albuquerque, NM, USA 87185*
[2] *Department of Mechanical and Aerospace Engineering, University of Virginia, 122 Engineer's Way, Charlottesville, VA, USA 22904*
pehopki@sandia.gov

Abstract: Phonon scattering at boundaries drives the thermal transport in nanosystems. In this work, I will discuss various projects in which solid boundaries and interfaces are used to reduce the thermal conductance in nanosystems. These studies include cross plane thermal conductivity in periodic, porous silicon films and thermal boundary conductance across random and quantum dot roughened Si interfaces.

Successful reduction of the thermal conductivity in nanosystems has been achieved through the alteration of structure and interface density in different types of nanoparticle films and periodic composites.[1] These material systems have attracted significant attention due to their unique phonon-scattering mechanisms, where the increase in the density of inclusions increases the number and frequency of boundary scattering events, in turn resulting in lower realized values of effective thermal conductivity. Thus, through varying the frequency and strength of phonon scattering at interfaces, one is able to obtain a unique method for controlling the effective thermal conductivity of a given nanosystem.

In this work, I will review various projects in which we have studied thermal transport in nanosystems with periodic and structurally variant boundaries to reduce and control thermal transport. First, I will discuss recent measurements of the cross plane transport in periodically patterned porous silicon membranes; these silicon membranes are low frequency phononic crystals and we study the effects of coherent and incoherent mechanisms contributing to the cross plane thermal conductivity.[2] Secondly, I will review various projects in which structurally variant solid interfaces are used to decrease the thermal boundary conductance.[3,4] We show that roughening is an effective tool to systematically decrease the thermal boundary conductance. Finally, I will discuss recent measurement of thermal boundary conductance across silicon interfaces with quantum dot patterning. We show that quantum dot synthesis is an effective tool to control the thermal conductance in nanosystems due to phonon scattering and attenuation effects around the quantum dots.

We measure the thermal processes in the various nanosystems presented in this work with time domain thermoreflectance (TDTR).[5,6] TDTR is a non-contact, pump-probe technique in which a modulated train of short laser pulses (in our case ~ 100 fs) is used to create a heating event (pump) on the surface of a sample. This pump-heating event is then monitored with a time-delayed probe pulse. The change in the reflectivity of the probe pulses at the modulation frequency of the pump train is detected through a lock-in amplifier; this change in reflectivity is related to the temperature change on the surface of the sample. Details of the specific experimental setup at Sandia National Laboratories and the thermal analysis used to determine thermal conductivity and thermal boundary conductance is discussed elsewhere.[7]

Figure 1 shows the the thermal conductivity of periodically porous Si structures at room temperature as a function of the characteristic limiting distance, L, for the phononic crystal patterns (unfilled squares – numbers represent hole diameters/pitch in hundreds of nanometers), microporous solids (filled pentagons),[8] and nanomesh (filled diamond).[9] The measured thermal conductivities are multiplied by a factor of $\left[\left(1+2\phi/3\right)/\left(1-\phi\right)\right]$ to account for the porosity of the structures, and thereby directly compare the thermal conductivity of the solid matrix in the porous structures to a model accounting for phonon boundary scattering and thermal conductivity in porous solids.[10] The solid line represents predictions of this model at room temperature as a function of L. This model predicts the thermal conductivity of the microporous solids well. This model, however, overpredicts the porous silicon measurements. The dashed line represents predictions of the porous silicon thermal conductivity, which accounts for a change in mode density using a plane wave expansion method.[11]

Phononics 2011: First International Conference on Phononic Crystals, Metamaterials and Optomechanics
Santa Fe, New Mexico, USA, May 29-June 2, 2011
PHONONICS-2011-0080

Figure 2 shows the measured thermal boundary conductance, h, as a function of surface roughness, δ, for a series of Al/Si samples. We roughen the Si interfaces via tetramethyl ammonium hydroxide (TMAH) solution at 80°C for various times to induce different degrees of Si surface roughness. We also treat a series of the Si surfaces with buffered oxide etch immediately before Al deposition to minimize the oxide layer at the interface. The thermal boundary conductances show a dependency on δ, which is not predicted by the traditional diffuse mismatch model.[12] We develop a new model that accounts for thermal conductance at rough interfaces and oxide formations, as shown by the solid lines in Fig. 2. Based on these results at the roughened Al/Si interfaces, we patterned a series of samples with Ge_xSi_{1-x} quantum dots on a Si surface and studied the thermal transport across Al/Si interfaces with quantum dot roughened surfaces. The measured thermal boundary conductance decreases with increased RMS roughness induced from the quantum dots, and our model for thermal boundary conductance across rough interfaces predicts the measured values well. The precise quantum dot patterning yields a method to control the thermal transport.

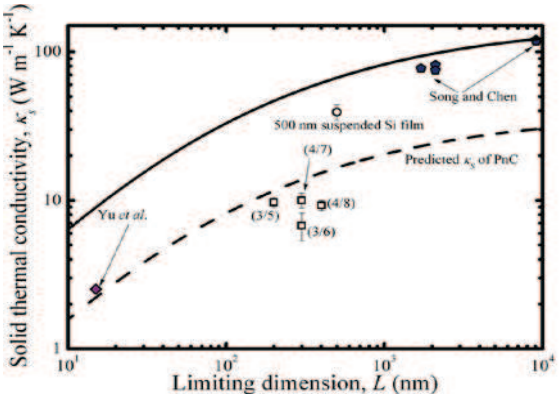

Figure 1. (see Ref. 2)

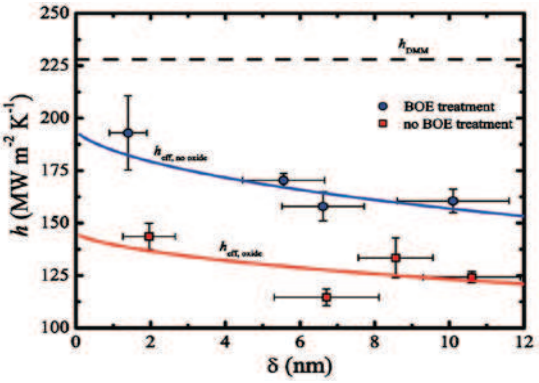

Figure 2. (See Ref. 4)

Acknowledgements
I would like to thank my collaborators on these various projects. I am greatly appreciative for funding from the LDRD Program Office through the Harry S. Truman Fellowship Program. This work was performed, in part, at the Center for Integrated Nanotechnologies, a U.S. Department of Energy, Office of Basic Energy Sciences user facility; the authors would like to thank John Sullivan for assistance regarding work at the Center for Integrated Nanotechnologies. Sandia National Laboratories is a multi-program laboratory operated by Sandia Corporation, a wholly owned subsidiary of Lockheed Martin Corporation, for the United States Department of Energy's National Nuclear Security Administration under Contract DE-AC04-94AL85000.

References
[1]D. G. Cahill, W. K. Ford, K. E. Goodson, G. D. Mahan, A. Majumdar, H. J. Maris, R. Merlin and S. R. Phillpot, J. Appl. Phys. **93**, 793 (2003).
[2]P. E. Hopkins, C. M. Reinke, M. F. Su, R. H. Olsson I I I, e. A. Shaner, Z. C. Leseman, J. R. Serrano, L. M. Phinney and I. El-Kady, Nano Letters **ASAP**, 10.1021/nl102918q (2010).
[3]P. E. Hopkins, P. M. Norris, R. J. Stevens, T. Beechem and S. Graham, J. Heat Transfer **130**, 062402 (2008).
[4]P. E. Hopkins, L. M. Phinney, J. R. Serrano and T. E. Beechem, Phys. Rev. B **82**, 085307 (2010).
[5]D. G. Cahill, K. E. Goodson and A. Majumdar, J. Heat Transfer **124**, 223 (2002).
[6]D. G. Cahill, Review of Scientific Instruments **75**, 5119 (2004).
[7]P. E. Hopkins, J. R. Serrano, L. M. Phinney, S. P. Kearney, T. W. Grasser and C. T. Harris, J. Heat Transfer **132**, 081302 (2010).
[8]D. Song and G. Chen, Appl. Phys. Lett. **84**, 687 (2004).
[9]J.-K. Yu, S. Mitrovic, D. Tham, J. Varghese and J. R. Heath, Nature Nanotechnology **5**, 718 (2010).
[10]P. E. Hopkins, P. T. Rakich, R. H. Olsson I I I, I. El-Kady and L. M. Phinney, Appl. Phys. Lett. **95**, 161902 (2009).
[11]M. S. Kushwaha, P. Helevi, G. Martinez, L. Dobrzynski and B. Djafari-Rouhani, Phys. Rev. B **49**, 2313 (1994).
[12]E. T. Swartz and R. O. Pohl, Reviews of Modern Physics **61**, 605 (1989).

Phononics 2011: First International Conference on Phononic Crystals, Metamaterials and Optomechanics
Santa Fe, New Mexico, USA, May 29-June 2, 2011
PHONONICS-2011-0081

Thermal conductance behavior of self-assembled lamellar block copolymer thin films

Matthew C. George, Patrick E. Hopkins, Mark A. Rodriguez

Sandia National Laboratories, PO Box 5800 Albuquerque, NM 87185, USA
mcgeorg@sandia.gov, pehopki@sandia.gov, marodri@sandia.gov

Abstract: We measure the thermal conductance of both disordered and self-assembled lamellar polystyrene-block-poly(methyl methacrylate) copolymer films and compare the results to literature reports on thin homopolymer films and polymer brushes. We see a 150% increase in thermal conductivity for a single self-assembled PS-b-PMMA layer.

The control of nano-scale phonon/thermal transport properties is a growing technical challenge in the fields of thermoelectrics, integrated circuits, and high power density lasers. Of particular importance in microelectronics packaging and integrated circuit thermal management are polymer and polymer composite films in the form of encapsulants and coupling compounds. Chain alignment has been shown to affect thermal transport in drawn polymers, polymer brushes, and self-assembled monolayers. In this work we examine the thermal conductance behavior of thin self-assembled block copolymer films. In particular we examine both ordered and disordered copolymer films of polystyrene-block-poly(methyl methacrylate) (PS-b-PMMA) and compare the results to literature reports on thin homopolymer films, polymer brushes, and bulk drawn homopolymers. Figure 1 depicts the sample configuration in which *n* is the number of lamellar periods in the ordered films. Previous reports typically show a modest increase in axial thermal conductivity (10-50%) for elongated PMMA polymer chains compared to random coil chain configurations. We see up to a 150% increase in thermal conductivity for a single self-assembled layer of PS-b-PMMA. Increasing the film thickness in a stepwise fashion to incorporate additional self-assembled layers of block copolymer decreased the thermal conductivity towards that of the amorphous state, which is close to reported values for the individual homopolymers (0.17 and 0.20 $Wm^{-1}K^{-1}$ for PS and PMMA respectively)[1].

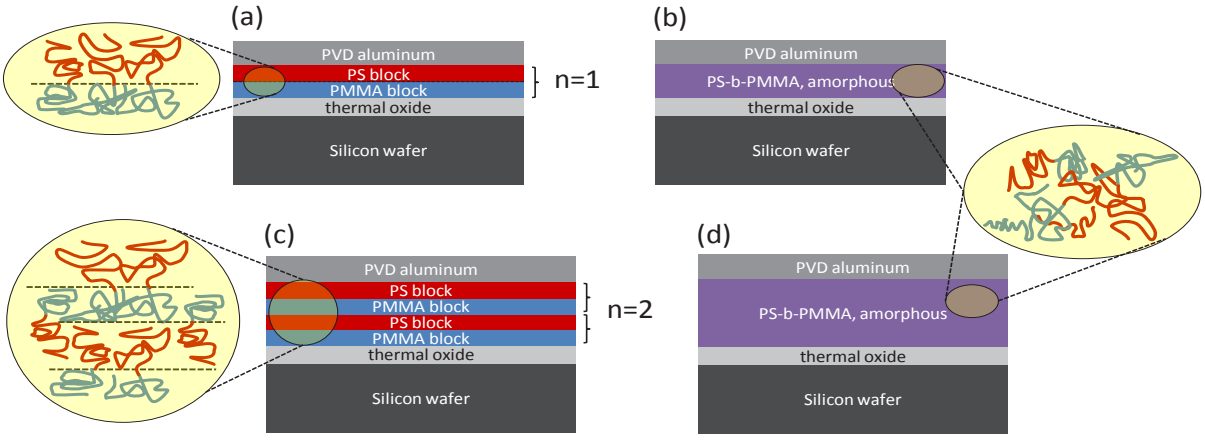

Figure 1 Schematic of ordered **(a)**, **(c)** and disordered **(b)**, **(d)** block copolymer thin films of PS-b-PMMA coated with aluminum via physical vapor deposition (PVD) on a thermal oxide silicon substrate. The number of lamellar periods is denoted by *n*. Exploded insets depict expected polymer chain conformation.

The PS-b-PMMA films were spun-cast from toluene solutions to thickness values commensurate with the natural lamellar period of the block copolymer. Film thickness was verified with ellipsometry. The spun-cast films are initially amorphous, but one set is annealed in a vacuum oven below the order-disorder transition temperature to promote self-assembly into the lamellar phase, which is aligned to the film substrate due to preferential segregation of PMMA to the polar thermal oxide surface, and PS to the vacuum interface[2-4]. The assembly of the annealed films into the stacked lamellar form as depicted in figure 1a and 1c was verified with X-ray reflectivity measurements. Rocking curves were

Phononics 2011: First International Conference on Phononic Crystals, Metamaterials and Optomechanics
Santa Fe, New Mexico, USA, May 29-June 2, 2011
PHONONICS-2011-0081

also collected to detect off-specular (diffuse) scattering in order to compare the in-plane film homogeneity. We measured the thermal conductivity of the lamellar and amorphous copolymer films with TDTR[5,6]. TDTR is a non-contact, pump-probe technique in which a modulated train of short laser pulses (in our case ~ 100 fs) is used to create a heating event (pump) on the surface of a sample. This pump-heating event is then monitored with a time-delayed probe pulse. The change in the reflectivity of the probe pulses at the modulation frequency of the pump train is detected through a lock-in amplifier; this change in reflectivity is related to the temperature change on the surface of the sample. This temporal temperature data is related to the thermophysical properties of the sample of interest. We monitor the thermoreflectance signal over 4.0 ns of probe delay time. We deposit a 90 nm Al film on the samples as a transducer that relates the measured reflectivity to the temperature change on the surface. The deposited energy takes approximately 100 ps to propagate through the Al layer, and the remaining delay time is related to the heat flow across the copolymer films and the thermal diffusivity in the underlying substrate. Our specific experimental setup is described in detail elsewhere[7]. The thermoreflectance signal we monitor is the ratio of the in-phase to the out-of-phase voltage recorded by the lock-in amplifier, which is related to the temperature change on the surface of the sample. The thermal model and analysis used to predict the temperature change and subsequent lock-in ratio is described in detail in the references[7]. We assume bulk values for the thermophysical properties of the Al, SiO_2, and Si,[8] and we verify the Al film thickness via picosecond ultrasonics[9,10].

The measured thermal conductivity of our copolymer films is depicted in Fig. 2 along with the thermal conductivity of spun cast polymer films and brushes[11]. The ordered films exhibit a higher thermal conductivity than the disordered films, with the thermal conductivity decreasing as the number of block copolymer layers was increased. For the single period, ordered PS-b-PMMA film, we believe preferential polymer chain alignment parallel to the film normal is the main factor accounting for the increased out of plane thermal conductivity. This is likely due to the increased anisotropy and effectiveness of intra-chain thermal transport, whereby vibrations are transmitted along the covalent bonds of the polymer backbone. Increasing the number of periods *n*, or reducing the film order, results in more inter-chain thermal transport, in which vibrations must be transferred through weaker van der Waals and dipole interactions[12]. In addition to partial chain alignment, we suspect that boundary scattering and phonon-phonon scattering are also contributing factors to the observed behavior.

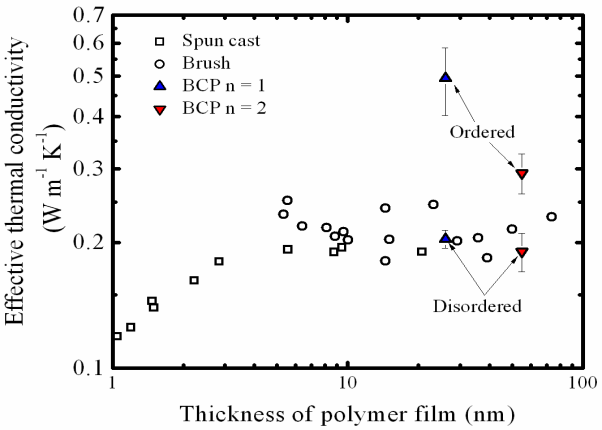

Figure 1 Thermal conductivity of our block copolymer (bcp) films compared to that of spun-cast PMMA films and polymer brushes[11]. The ordered films exhibit a higher thermal conductivity than the disordered films, spun-cast films, and brushes.

References

[1] H. Lee, *Rev. Sci. Instrum.* **53**, 884 (1982).
[2] G.H. Fredrickson, *Macromolecules* 20, 2535 (1987)
[3] A. Menelle, T.P. Russell, S.H. Anastasiadis, S.K. Satija, C.F. Majkrzak, *Phys. Rev. Lett.* **68**, 67 (1992)
[4] H. Hasegawa, T. Hashimoto, *Macromolecules* **18**, 589 (1985)
[5] D.G. Cahill, K.E. Goodson and A. Majumdar, *J. Heat Transfer* **124**, 223 (2002).
[6] D.G. Cahill, *Rev. Sci. Instrum.* **75**, 5119 (2004).
[7] P.E. Hopkins, J. R. Serrano, L.M. Phinney, S.P. Kearney, T.W. Grasser, C.T. Harris, *J. Heat Transfer* **132**, 81302 (2010).
[8] F. Incropera and D.P. DeWitt, *Fundamentals of Heat and Mass Transfer*, Wiley and Sons, Inc., New York, (1996).
[9] C. Thomsen, H.T. Grahn, H.J. Maris and J. Tauc, *Phys. Rev. B* **34**, 4129 (1986).
[10] C. Thomsen, J. Strait, z. Vardeny, H.J. Maris, J. Tauc and J.J. Hauser, *Phys. Rev. Lett.* **53**, 989 (1984).
[11] M.D. Losego, L. Moh, K.A. Arpin, D.G. Cahill and P.V. Braun, *Appl. Phys. Lett.* **97**, 011908 (2010).
[12] D. Yorifuji, S. Ando, *Macromolecules* **43**, 7583 (2010)

* A portion of this work was supported by the Laboratory Directed Research and Development program at Sandia National Laboratories. Sandia is a multiprogram laboratory operated by Sandia Corporation, a Lockheed Martin Company, for the United States Department of Energy's National Nuclear Security Administration under Contract DE-AC04-94AL85000.

Phononics 2011: First International Conference on Phononic Crystals, Metamaterials and Optomechanics
Santa Fe, New Mexico, USA, May 29-June 2, 2011
PHONONICS-2011-0088

Low-Temperature Thermal Conductance of Periodically Perforated Silicon Nitride Membranes

N. Zen[1], T. J. Isotalo[1], I. J. Maasilta[1]

[1] *Nanoscience Center, University of Jyväskylä, Finland*
nobuyuki.zen@jyu.fi, ilari.j.maasilta@jyu.fi

Abstract: In order to enhance the thermally insulating propertiy of a silicon nitride (Si_3N_4) membrane, we have micromachined periodic holes through it with the intent of producing a complete phononic bandgap. The observation of the thermal transport in the phononic crystal is carried out by using a well-established Normal metal-Insulator-Superconductor (NIS) tunnel junction thermometer at sub-Kelvin temperatures. In addition, numerical calculations of the thermal conductance of the structure are in progress.

Periodically Perforated Si_3N_4 Membrane as a Phononic Crystal

Phononic crystals are promising devices[1] for ultrasonic sensors, acoustic filters or waveguides, as well as high efficient thermoelectric transducers, and the next-generation ultra high sensitive superconducting radiation detectors, whose performance strongly depend on the phonon thermal conductance. Because the superconducting detectors convert the energy of the photons[2] or proteins[3] from the Time-Of-Flight Mass Spectrometer (TOF MS) into phonons, it is important to mount the detector on the infrastructure which can enclose phonons and prevent them from dissipating to surroundings too quickly. A silicon nitride (Si_3N_4) membrane is frequently used material for this purpose because of its low thermal conductivity and the ease of controlling its dimension and structure[2]. In order to enhance the sensitivity of the superconducting detectors, we have started developing periodically perforated Si_3N_4 membranes which are expected to perform as phononic crystals. Using finite element method based calculations (COMSOL Multiphysics), we have successfully found the proper geometry which has a complete phononic bandgap extended from 17.7 GHz to 22.0 GHz, as shown in Figure 1 (a). For the 3-D Debye model, the dominant thermal phonon frequency at a temperature T is expressed as $\omega = 2.8k_BT/\hbar$. In our case, however, the perforated-membrane structure has only in-plane periodicity, therefore we should compare the bandgap with the 2-D Debye model, whose dominant thermal frequency is expressed as $\omega = 1.5k_BT/\hbar$. At the temperature of 100 mK, it corresponds to $\omega = 20$ GHz, just in the middle of the complete bandgap of Figure 1. Hence, we can expect the suppression of the thermal conductance in our modeled geometry. Moreover, the simulation of the constant energy surface in Figure 1 (b) shows that the perforated membrane exhibits a strong directionality in the thermal transport, which is isotropic in the case of the unperforated membrane in Figure 1 (c). This effect, known as phonon focusing in regular crystals[4] will also contribute to the thermal properties of the membrane.

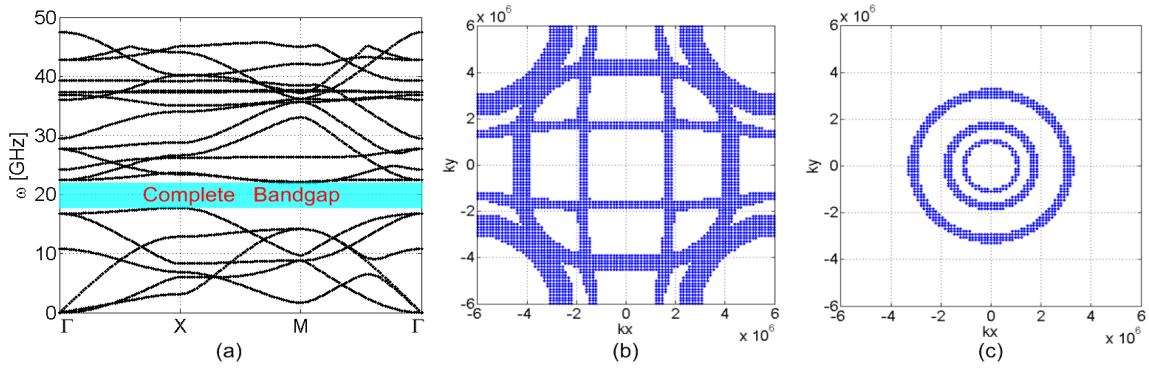

Figure 1 (a) A dispersion relation of the perforated Si_3N_4 membrane, calculated by COMSOL Multiphysics with the Matlab environment. The complete bandgap extends from 17.7 GHz to 22.0 GHz. **(b)** Constant energy surface of the perforated Si_3N_4 membrane and **(c)** unperforated membrane at the frequency of 10 GHz in k_x, k_y space.

Phononics 2011: First International Conference on Phononic Crystals, Metamaterials and Optomechanics
Santa Fe, New Mexico, USA, May 29-June 2, 2011
PHONONICS-2011-0088

NIS Tunnel Junction Thermometry for Phonons

In order to investigate phononic thermal conduction, we have been using the Normal metal-Insulator-Superconductor (NIS) tunnel junctions as thermometers[5,6]. A SEM image of a NIS thermometer and its operating circuit is shown in Figure 2 (a). NIS junctions are fabricated using an electron-beam lithography and an ultra-high-vacuum e-beam evaporation. A typical size of the junction is a several hundreds of nm each as in the inset of Figure 2 (a). The red part in the figure (online) is a normal metal (Cu) island which can absorb phonons from the environment. The thermometer works with a constant-current bias, with the voltage being inversely proportional to the normal metal electron temperature[5,6]. As the superconducting leads (Al) of the NIS junctions do not carry any heat electronically, all the absorbed and emitted power is carried by phonons. In this dynamic equilibrium case, the electron temperature follows the phonon temperature. The sensitivity of the NIS thermometer is extremely high as much as 0.9 μV/mK below 200 mK. The small length of the island of the order of μm is also suitable for measuring the local phonon temperature.

Figure 2 (c) is a dark-field micrograph of a perforated Si_3N_4 membrane of the thickness of 300 nm with a hole diameter of 5 μm and a lattice constant of 10 μm. Two SINIS junctions located at the center act as a thermometer and a heater, respectively. Holes are uniformly formed across the whole membrane size of 360 × 360 μm^2.

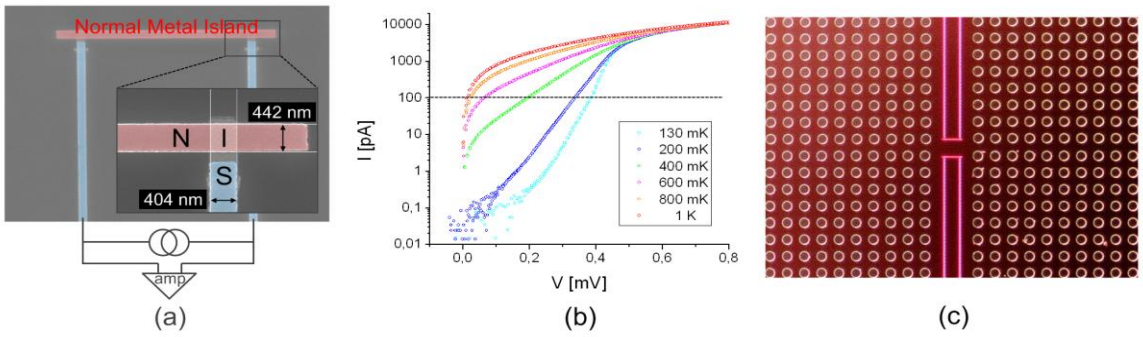

Figure 2 (a) A SEM image of the NIS thermometer and its operating circuit. NIS thermometers are operated by a constant-current biasing. **(b)** *I-V* characteristics of the NIS thermometer at various temperatures. **(c)** A dark-field micrograph of the perforated Si_3N_4 membrane with a SINIS thermometer and a heater.

References

[1] Y. Pennec, J. O. Vasseur, B. Djafari-Rouhani, L. Dobrzynski, and P. A. Deymier, *Surface Sci. Reports* **65**, 229-291 (2010).
[2] C. Enss, *Cryogenic Particle Detection*, Springer, Germany (2005).
[3] A. Casaburi, M. Ejrnaes, N. Zen, M. Ohkubo, S. Pagano, and R. Cristiano, *Appl. Phys. Lett.* **98**, 023702 (2011).
[4] J. P. Wolfe, *IMAGING PHONONS*, Cambridge University Press, UK (1998).
[5] J. T. Karvonen, and I. J. Maasilta, *Phys. Rev. Lett.* **99**, 145503 (2007).
[6] P. J. Koppinen, and I. J. Maasilta, *Phys. Rev. Lett.* **102**, 165502 (2009).

Phononics 2011: First International Conference on Phononic Crystals, Metamaterials and Optomechanics
Santa Fe, New Mexico, USA, May 29-June 2, 2011
PHONONICS-2011-0094

Dispersion of Confined Acoustic Phonons in Ultra-Thin Si Membranes

J. Cuffe[1,2], E. Chavez[2,3], P-O. Chapuis[4], E. H. El Boudouti[4,5], F. Alzina[2], D. Dudek[2], Y. Pennec[5], B. Djafari-Rouhani[5], A. Shchepetov[6], M. Prunnila[6], J. Ahopelto[6], C. M. Sotomayor Torres[2,7]

[1] Dept. of Physics., University College Cork, Tyndall National Institute, Prospect Row, Cork, Ireland
[2] Catalan Institute of Nanotechnology (ICN-CIN2), Campus UAB, 08193 Bellaterra (Barcelona), Spain
[3] Dept. of Physics, UAB, 08193 Bellaterra (Barcelona), Spain
jcuffe@icn.cat,echavez@icn.cat,olivier.chapuis@cin2.es,francesc.alsina.icn@uab.es,clivia.sotomayor@icn.cat
[4] Institut d'Electronique, de Microélectronique et de Nanotechnologie (IEMN), Université de Lille 1, France
yan.pennec@univ-lille1.fr, bahram.djafari-rouhani@univ-lille1.fr
[5] LDOM, Faculté des Sciences, Université Mohamed 1, Oujda, Morocco
[6] VTT Technical Research Centre of Finland, PO Box 1000, 02044 VTT, Espoo, Finland
Jouni.Ahopelto@vtt.fi, Andrey.Shchepetov@vtt.fi,Mika.Prunnila@vtt.fi,
[7] Institució Catalana de Recerca i Estudis Avançats (ICREA), 08010 Barcelona, Spain

The dispersion curves of confined acoustic phonons in ~10 and ~30 nm Si membranes were measured using Brillouin Light Scattering (BLS) spectroscopy. The dispersion relations of the confined phonons were calculated from a semi-analytical model based on continuum elasticity theory. Green's function simulations were used to simulate the Brillouin spectra.

The acoustic properties of ultra-thin Si layers are important for many areas of nanofabrication, impacting on both structural integrity and thermal transport. The effect of phonon confinement is particularly important, affecting both heat dissipation and charge carrier mobility[1,2]. The goal of this work is to obtain a deeper understanding of phonon confinement and propagation in materials with dimensions comparable to thermal phonon wavelengths. Previous studies have investigated out-of-plane confined acoustic phonons in 30 nm Si membranes by inelastic light scattering at normal incidence, with use of a triple grating Raman spectrometer[3,4]. In this work the in-plane propagation of these modes is investigated as a function of the parallel component of the wavevector, using a high-resolution Tandem Fabry-Perot Interferometer. The effect of the ~1 nm native oxide layer in such thin systems was also calculated using a three-layer model.

Methods

Brillouin Light Scattering (BLS) spectroscopy is an inelastic light scattering technique, which can directly measure acoustic phonon dispersion in a non-destructive manner. Using an angle-resolved approach, out-of-plane confined phonons as well as flexural, dilatational, and shear modes propagating in the plane of the membrane were investigated. The dispersion curves were calculated from numerical solutions to the analytic equations for the acoustic modes in a membrane, based on a continuum elasticity model[5]. Green's function simulations were also used to calculate the density of states of the phonon modes and to simulate the Brillouin spectra[6]. The membranes of area 500 x 500 μm^2 were fabricated on nominally undoped 150 mm thin SOI wafers using Si MEMS processing techniques. The thin SOI wafers were produced by bonding the standard SOI wafers from SOITEC company[7] with a Si oxidized wafers.

Results

The BLS spectra of the membranes corresponded to calculated thicknesses of 12 and 28 nm. Calculations for the 12 nm membrane showed that mode frequencies exhibit a detectable shift of 8% with changes in the thickness of the membrane of 1 nm, which is of the order of the uncertainty in the thickness measurement. The ultra-thin nature of the membranes resulted in a slow phase and group velocity for the first order flexural (A0) modes, with a phase velocity down to 320 m s^{-1} recorded for the 12 nm membrane. This is 15 times smaller than the comparable bulk value (Rayleigh Wave)

v_{RSAW} = 4921 m s^{-1}. This resulted in a large phonon density of states, as evidenced by an enhanced acousto-optic interaction and therefore a strong scattered signal. It was observed that the experimental

Phononics 2011: First International Conference on Phononic Crystals, Metamaterials and Optomechanics
Santa Fe, New Mexico, USA, May 29-June 2, 2011
PHONONICS-2011-0094

data agree with the dispersion curves calculated from continuum elasticity theory to within experimental error, apart from the dilatational mode of the 12 nm membrane (Figure1a), which is under further investigation.

Calculations for a three layer system were also performed to take account of the native oxide layer, which was found to cause a detectable change in the dispersion of the higher order (n>0) acoustic modes. (Figure 1b)

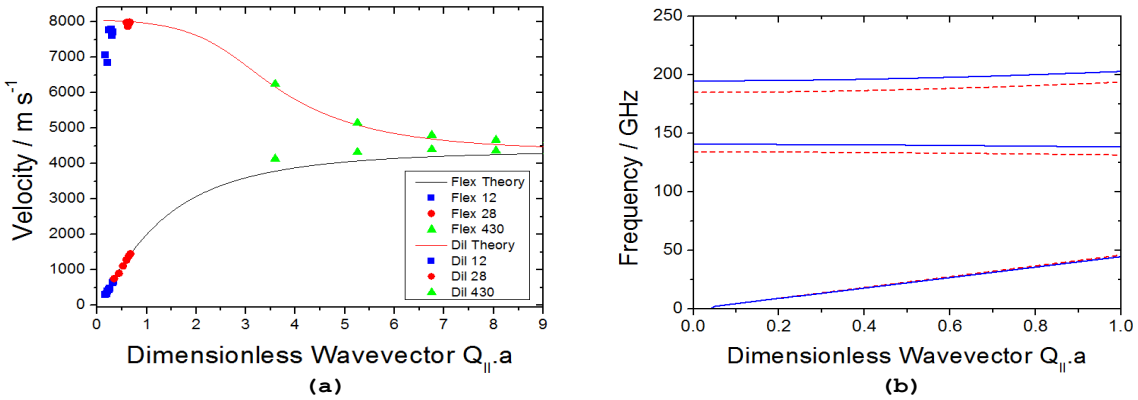

Fig. 1: (a) Phase velocity vs. dimensionless parallel wavevector for 12 nm (blue squares), 28 nm (red circles) and 430 nm (green triangles) membranes, with theoretical calculations for the first order flexural (black line) and dilatational (red line) modes of a Si membrane. (b) : Dispersion curves of the dilatational modes of a 30 nm Si membrane, (blue solid line) and 28.4nm Si with 1.6 nm SiO2 on the top and bottom surfaces (red dashed line).

Conclusions

The acoustic dispersion relations of confined phonons in ultra-thin Si membranes, with thicknesses of 12 and 28 nm, were measured. The experimental results were compared with semi-analytic and Green's function calculations with satisfactory agreement, confirming a small phase and group velocity for the first order flexural mode. Calculations show that the spectra are sensitive to changes in thickness of the membrane on the order of 1 nm. The higher order acoustic modes were also shown to be sensitive to the presence of the thin native oxide layer. This work provides a basis to investigate the effect of acoustic phonon confinement on thermal transport in systems with sub- 50 nm dimensions.

Acknowledgements

The authors are grateful for financial support from the FP7 projects ICT FET TAILPHOX (grant nr. 233883), ICT IP NANOPACK (grant 216176) and the MICINN project ACPHIN (FIS2009-10150). J.C. gratefully acknowledges financial support under an Irish Research Council for Science, Engineering, and Technology (ICRSET) scholarship.

References

[1] L. Donetti, F. Gamiz, J. B. Roldan and A. Godoy, *J. App. Phys.*,**100**, 013701 -013701-7 (2006)
[2] Huang, M.-J.; Chang, T.-M.; Chong, W.-Y.; Liu, C.-K. & Yu, C.-K.*Int. J. of Heat and Mass Transfer,* **2007**, *50*, 67 - 74
[3] C. M. Sotomayor-Torres, A. Z. F. Poinsotte, J. Groenen, M. Prunnila, J. Ahopelto, A. Mlayah and V. Paillard, *Physica Status Solidi (C), **1**(11)*, 2609-2612 (2004)
[4] J. Groenen, F. Poinsotte, A. Zwick, C. M. Sotomayor-Torres, M. Prunnila and J. Ahopelto, *Phys. Rev. B*, **77**, 045420 (2008)
[5] Lamb, H. *Proc. Lond. Math. Soc*. **93** 114 (1917)
[6] E. H. El Boudouti, B. Djafari-Rouhani, A. Akjouj, and L. Dobrzynski, *Surface Science Reports*, **64**, 471 – 594 (2009)
[7] M. Bruel, B. Aspar, and A. J. Auberton-Herve, *Jpn. J. Appl. Phys., Part 1 **36***, 1636 (1997)

Phononics 2011: First International Conference on Phononic Crystals, Metamaterials and Optomechanics
Santa Fe, New Mexico, USA, May 29-June 2, 2011
PHONONICS-2011-0103

Acoustic Phonon Transmission and Heat Conduction Through Vacuum

Mika Prunnila, Johanna Meltaus

VTT Technical Research Centre of Finland, P.O.Box 1208, FIN-02044 VTT, Espoo,Finland
mika.prunnila@vtt.fi, johanna.meltaus@vtt.fi

Abstract: We describe theoretically how acoustic phonons can directly transmit energy and conduct heat between bodies that are separated by a vacuum gap. This effect is enabled by introducing a coupling mechanism, such as piezoelectricity, that strongly couples electric field and lattice deformation.

Advances in experimental techniques have enabled near-field heat transfer measurements from μm down to 10 nm body distances[1]. We have recently proposed that at such distances a new type of evanescent field heat transfer mechanism due to acoustic phonons can exist[2]. Significant energy transmission and heat flux across a vacuum gap is possible if the acoustic phonons can induce a quasi-static electric field, which then can leak into the vacuum [see Figs. 1(a) and 1(b)]. Such a mechanism is provided, for example, by the piezoelectric (PE) effect.

Our approach involves the determination of the scattering matrix of the system and the resulting energy transmission coefficients T_γ.[2] The thermal boundary conductance G_γ arising from transmission of mode γ is calculated by phonon Landauer formula, which we write in the form

$$G_\gamma = \frac{2\pi^2}{30} v_\gamma k_B q_T^3 \left(1 + \frac{q_T}{4}\frac{\partial}{\partial q_T}\right) T_\gamma^{eff} \tag{1}$$

$$T_\gamma^{eff} = \frac{15}{\pi^4}\left\langle \int_0^{q_c/q_T} dx \frac{x^3}{e^x - 1} T_\gamma(q_T d, \theta, \phi) \right\rangle, \tag{2}$$

where T_γ^{eff} is the effective transmission coefficient, v_γ is phonon velocity and $q_T = 2\pi k_B T/\hbar v_\gamma$ is the thermal wave number (T being the temperature). Mode indices $\gamma=L$ and $\gamma=S$ stand for longitudinal and transversal, respectively (the two transversal modes are not written explicitly). Here q_c is the Brillouin/Debye cut-off and <…> stands for solid angle average.

Coupling of lattice deformation and (quasistatic) evanescent electric field leads to certain type of scattering matrix and energy transmission without specifying the details of the (linear) coupling mechanism. This general analysis anticipates exponentially low "tunneling" regimes and also strong resonances in solid-vacuum-solid phonon transmission[2]. Here the numerical transmission calculation examples rely on piezoelectric coupling and, therefore, show some similarities with Refs. 3.

Figure 2(a) shows numerically calculated energy transmission T_γ from a PE material to another across a vacuum gap following the S-matrix approach of Ref. 2. We have adopted material parameters that are close to that of ZnO with the simplifying approximation of only one nonzero element of the piezo tensor (e_{33} = 1.3 C/m^2). Note that for this approximation the acoustic and electric fields are decoupled for the transversal mode whose polarization is parallel to the interfaces. Therefore, in Figure 2 the S mode refers to the mode whose polarization is in the plane of incidence and we need to consider only single angular variable θ, the angle of incidence. We can observe that the transmission probability of both modes exhibit strong resonances in the (qd,θ)-plane. Most striking feature is that at/around the resonances the phonons can go through the gap with (or close to) unity transmission.

Figure 2(b) shows T_γ^{eff} and G_γ obtained from Eqs. (1) and (2) and T_γ of Fig. 2(a). At low temperatures the S-mode thermal conductance G_S is ~15 % of the unity transmission thermal conductance. At high temperatures G_S saturates, because only long wavelength transversal phonons can go across the gap.

Phononics 2011: First International Conference on Phononic Crystals, Metamaterials and Optomechanics
Santa Fe, New Mexico, USA, May 29-June 2, 2011
PHONONICS-2011-0103

The L-mode shows no saturation, because of the strong resonances at large q. These resonances enable some of the small wavelength longitudinal phonons to be transmitted across the vacuum gap even with unity transmission. It should be noted that if we introduce a finite cutoff q_c then G_L also saturates at the limit $q_T / q_c >> 1$.

We conclude that, essentially, this work describes how acoustic phonons can directly transmit energy and heat between bodies without any mechanical inter-body contact. We believe that this novel effect is of interest in phononics and nanoscale heat transport.

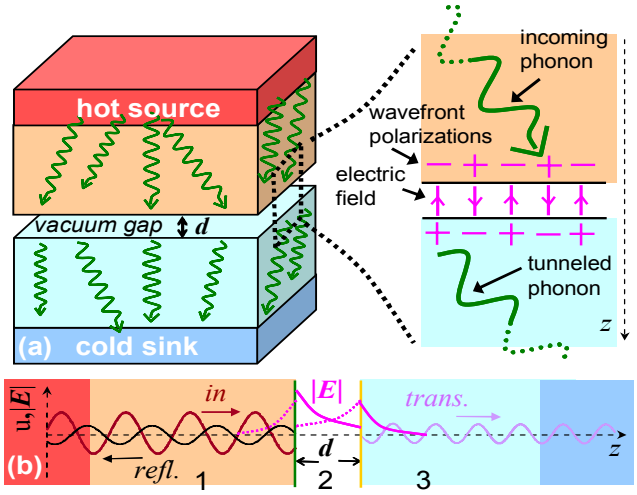

Figure 1 Illustration of the phonon transmission/tunneling effect through a vacuum gap. (a) Hot source radiates phonons towards cold sink. Single phonon carries an electric field, illustrated by + or - signs of wavefront polarization. The polarization induces an electric field into the vacuum gap. The field enables finite transmission over the gap. (b) A projection showing the spatial behaviour of the phonon waves (***u***) and of the evanescent electric ***E***. The dashed curves depict the "reflected" evanescent field.

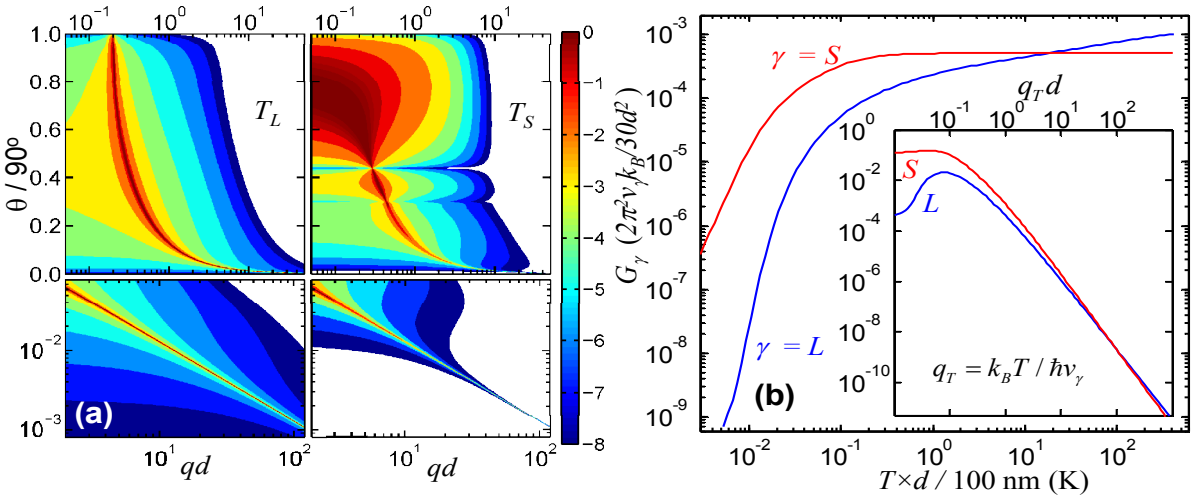

Figure 2 (a) Logarithmic contour plot of energy transmission coefficients T_γ between two PE bodies as a function of normalized wave vector qd (d is the gap width) and the angle of incidence θ. The lower panels show log-log blow-up of the small-θ large-qd region. **(b)** Effective transmission T_g^{eff} (the inset) as a function of $q_T d$ and the interface thermal conductance G_γ (the main part) as a function of temperature (we have set $q_c \to \infty$). The curves are obtained from the T_γ of (b) by using Eqs. (1) and (2). For the y-axis units of the main figure we have $2\pi^2 v_\gamma k_B / 30d^3 = Y_g \times (100\ \text{nm}/d)^3$ W/Km^2, where $Y_{L(S)}$ = 55.6 (24.9).

References

[1] See, for example, E. Rousseau *et al.*, Nature Photonics **3**, 514 (2009).
[2] M. Prunnila and J. Meltaus, Phys. Rev. Lett. **105**, 125501 (2010).
[3] M. K. Balakirev and A. V. Gorchakov, Sov. Phys. Solid State **19**, 355 (1977); M.K. Balakirev, S.V. Bogdanov, and A.V. Gorchakov, Sov. Phys. Solid State **20**, 338 (1978); Y. V. Gulyaev and V. P. Plesskii, Sov. Phys. Solid State **20**, 71 (1978).

Phononics 2011: First International Conference on Phononic Crystals, Metamaterials and Optomechanics
Santa Fe, New Mexico, USA, May 29-June 2, 2011
PHONONICS-2011-0104

Nanostructured two-dimensional phononic materials

K. Muralidharan[1], P.A. Deymier[1], N. Swinteck[1], K. Runge[1], and J-F. Robillard[2]

[1] *Department of Materials Science and Engineering, University of Arizona, Tucson, Arizona 85721, USA,*
krishna@email.arizona.edu, deymier@email.arizona.edu, swinteck@email.arizona.edu,
[2] *Institut d'Électronique, de Microélectronique et de Nanotechnologie, UMR CNRS 8520, Cité Scientifique, 59652 Villeneuve d'Ascq Cedex, France,*
jean-francois.robillard@isen.fr

Abstract: Phononic properties of nanostructured two-dimensional materials such as graphene and boron nitride (BN) sheets are calculated using the method of molecular dynamics. Nanophononic crystals composed of periodic array of holes in graphene exhibit Bragg scattering at non-cryogenic temperatures leading to reduction in thermal conductivity. The transport of phonons across non-periodic arrays of asymmetric holes in BN sheets is discussed in the context of scattering and non-linear effects that may lead to thermal rectification.

Phonons contributing to thermal conductivity have wavelengths ranging from nanometers to several hundreds of nanometers. Nanofabrication techniques have the potential of structuring materials in a way that may affect the propagation of thermal phonons. This possibility opens perspectives in the fields of thermal management and thermoelectrics. Modulating the thermal properties by creating a nanoscale composite material is an approach that has been extensively studied in the case of superlattices [1-3]. These stacks of nanoscale layers have been shown theoretically and experimentally to impact thermal transport due to scattering effects of phonons. In contrast to the 1-D superlattice structures, not much is known of the effect of 2D nanophononic structures on thermal conductivity and phonon transport. In this work we report on the phononic properties of nanostructured two-dimensional materials such as graphene and boron nitride (BN) sheets. Specifically we examine periodically patterned anti-dot graphene structures and defected BN sheets. Thermal properties and phonon transport behavior are modeled using the method of molecular dynamics (MD). The forces between atoms are determined from Tersoff-Brenner family of interatomic potentials . Both equilibrium as well as non-equilibrium MD formulations are used in this work to examine thermal properties of the systems under study.

MD simulations are carried out in conjunction with phononic band structure calculations in order to characterize the thermal transport properties of graphene-based nanophononic crystals composed of periodic arrays of hole inclusions (Fig. 1). In particular, the heat current autocorrelation function is calculated using the Green-Kubo equilibrium method, enabling the estimation of the lifetimes of acoustical and optical phonons as well as the thermal conductivity as functions of the filling fraction of the phononic crystals and temperature (Figs. 2a and 2b). We observe that Bragg scattering of thermal phonons leads to dramatic changes in the phonon lifetimes for filling fractions as low as 2.5% over a significant range of temperature. This change of lifetimes is followed by a corresponding change in the thermal conductivity. We discuss the results on the phonon lifetime in the context of competition between elastic Bragg scattering and inelastic phonon-phonon scattering. Our results suggest that in addition to impacting elastic scattering, band effects due to the phononic structure may also impact inelastic scattering.

Boron nitride (BN) sheets and thin films can contain non-periodic distributions of triangular holes as shown in Ref [4]. Using non-equilibrium molecular dynamics methods, the thermal transport perpendicular to an array of triangular holes in a BN sheet (Fig. 2) is studied as a function of thermal gradient of variable magnitude and sign. Results indicate that there is asymmetry in the magnitude of thermal flux when the thermal gradient changes sign, due to the interplay between geometrical effects (phonon scattering by asymmetric holes) and non-linear effects such as temperature dependent phonon density of states. Further, asymmetry in thermal transport is observed over a broad range of temperatures. These effects suggest

Phononics 2011: First International Conference on Phononic Crystals, Metamaterials and Optomechanics
Santa Fe, New Mexico, USA, May 29-June 2, 2011
PHONONICS-2011-0104

that BN sheets containing oriented non-periodic triangular holes may serve as a platform for designing a thermal rectifier or thermal diode.

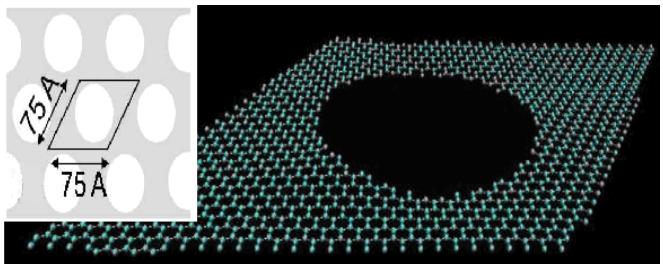

Figure 1: Illustration of the patterned graphene structure.

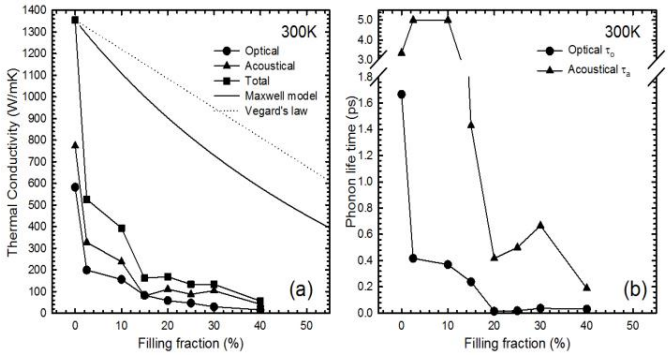

Figure 2: (a) Thermal conductivity deduced from the Green-Kubo method as a function of the filling fraction at 300 K (Squares). The contribution of the optical (Circles) and acoustical phonons (Triangles) are distinguished. These data are compared to a parallel (dotted line) and Maxwell (solid line) mixing model. (b) Mean acoustical and optical phonons lifetimes as a function of the filling fraction at 300K. These lifetimes are estimated from the fit of the heat current correlation functions. Error bars on calculated lifetime and thermal conductivity due to the exponential fit of the heat current autocorrelation functions are the size of the data points.

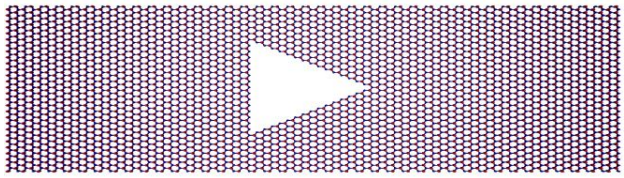

Figure 3: An illustration of the 2-D BN sheet with the triangular defect. The X-Y dimensions of the sheet are 175 Å x 70 Å, and periodic boundary conditions are employed in the Y direction, and the temperature gradients are applied in the X direction.

References

[1] P. Hyldgaard and G. D. Mahan, in *Thermal Conductivity*, Vol. 23, (Technomic, Lancaster, PA, 1996)
[2] G. Chen, C. L. Tien, X. Wu, and J. S. Smith, J. Heat Transfer **116**, 325 (1994)
[3] W. S. Capinski and H. J. Maris, Physica B **219**, 699 (1996)
[4] C. Jin, F. Lin, K. Suenaga, and S. Iijima, Phys. Rev. Lett. 102, 195505 (2009).

Phononics 2011: First International Conference on Phononic Crystals, Metamaterials and Optomechanics
Santa Fe, New Mexico, USA, May 29-June 2, 2011
PHONONICS-2011-0108

Effect of Interface Roughness on Phonon Transport in Superlattices

Kevin P. Pipe[1,2] and Huarui Sun[1]

[1]Department of Mechanical Engineering
[2]Department of Electrical Engineering and Computer Science
University of Michigan, Ann Arbor, MI, USA
pipe@umich.edu, hrsun@umich.edu

Abstract: We present a boundary perturbation method to analyze phonon reflection, transmission, and mode conversion at a rough interface, and extend these calculations using a transfer matrix approach to examine the effects of interface roughness on phonon transport in multilayer thin films.

Superlattices have been used to control the transport of acoustic phonons for coherent phonon[1,2] and heat transfer applications. In phonon "lasers" and terahertz phonon devices, superlattices are used as Bragg reflectors for acoustic cavities[3-5]. In thermoelectric devices, superlattices are used to increase phonon scattering and hence reduce thermal conductivity, leading to higher thermoelectric energy conversion efficiency[6-8].

Coherent effects that rely on interface periodicity, such as Bragg reflection, are sensitive to fluctuations in interface position caused by roughness. Interface roughness can disrupt specular interference effects, increase parasitic coupling into other phonon modes (e.g., longitudinal acoustic into transverse acoustic), and increase diffusive scattering. Since the acoustic phonons relevant for terahertz devices and most heat transfer applications have wavelengths less than 10 nm, atomic-scale interface roughness is expected to play a much more significant role than it does at optical wavelengths.

Previous work has examined the interaction of acoustic phonons with interface roughness by implementing an empirical specularity parameter[9-11] or by summing a collection of specular reflections off of a defined roughness geometry[12]. Such approaches are limited in their ability to account for phonon mode conversion at the interface. Lattice dynamics and Green's function formulations[13,14] have also been utilized for this purpose but are often computationally expensive and restricted to unrealistic roughness profiles (such as short in-plane correlation lengths).

We have developed a boundary perturbation method to model phonon transport at rough solid-solid interfaces, building off of previous work that has applied such methods to rough interfaces between liquid helium and copper[15,16] as well as ice and water[17]. This approach allows interface roughness to be characterized by statistical parameters such as the standard deviation of interface height (RMS roughness) and the in-plane correlation length, making calculations of mode conversion and separation into specular and diffuse components straightforward.

Using the boundary perturbation method, we predict the frequency (wavelength) and angle of transverse (TA) and longitudinal (LA) acoustic phonons emitted when an LA phonon is incident on a single rough interface at a particular angle. We then utilize these parameters within a transfer matrix approach to calculate the phonon transmission and reflection characteristics of a superlattice with a specified roughness profile. Metrics of interest for phonon Bragg reflectors (e.g., coherent reflectivity, full with at half maximum of the stop band) are calculated for superlattices in relevant material systems such as $SrTiO_3/BaTiO_3$ with various roughness profiles and numbers of superlattice periods. A quantitative analysis is performed to assess the relative contributions of acoustic impedance contrast and interface flatness to superlattice reflectivity. Implications for heat transfer applications (e.g., thermal boundary resistance) at low temperature are discussed.

This work was supported by the United States Air Force Office of Scientific Research (AFOSR) through the Multidisciplinary University Research Initiative (MURI) program under grant number FA9550-08-1-0340.

Phononics 2011: First International Conference on Phononic Crystals, Metamaterials and Optomechanics

Santa Fe, New Mexico, USA, May 29-June 2, 2011

PHONONICS-2011-0108

References

[1] N. M. Stanton, R. N. Kini, A. J. Kent, M. Henini, and D. Lehmann, *Phys. Rev. B* **68**, 113302 (2003).
[2] A. Bartels, T. Dekorsy, H. Kurz, and K. Köhler, *Phys. Rev. Lett.* **82**, 1044 (1999).
[3] M. Trigo, A. Bruchhausen, A. Fainstein, B. Jusserand, and V. Thierry-Mieg, *Phys. Rev. Lett.* **89**, 227402 (2002).
[4] A. J. Kent et al., *Phys. Rev. Lett.* **96**, 215504 (2006).
[5] P. A. Fokker, J. I. Dijkhuis, and H. W. de Wijn, *Phys. Rev. B* **55**, 2925 (1997).
[6] R. Venkatasubramanian, *Phys. Rev. B* **61**, 3091 (2000).
[7] M. N. Touzelbaev, P. Zhou, R. Venkatasubramanian and K. E. Goodson, *J. Appl. Phys.* **90**, 763 (2001).
[8] S.-M. Lee, David G. Cahill and R. Venkatasubramanian, *Appl. Phys. Lett.* **70**, 2957 (1997).
[9] J. M. Ziman, *Electrons and Phonons* (Oxford, 1960).
[10] G. Chen, *Phys. Rev. B* **57**, 14958 (1998)
[11] P. M. Norris and P. E. Hopkins, *J. Heat Transfer* **131**, 043207 (2009)
[12] A. Majumdar, *J. Heat Transfer* **113**, 797 (1991)
[13] B. C. Daly, H. J. Maris, K. Imamura and S. Tamura, *Phys. Rev. B* **66**, 024301 (2002)
[14] H. Zhao and J. B. Freund, *J. Appl. Phys.* **105**, 013515 (2009)
[15] A. D. Lapin, *Sov. Phys. Acoust.* **15**, 635 (1970).
[16] N. S. Shiren, *Phys. Rev. Lett.* **47**, 1466 (1981).
[17] W. A. Kuperman, *J. Acoust. Soc. Am.* **86**, 1511 (1989).

Phononics 2011: First International Conference on Phononic Crystals, Metamaterials and Optomechanics
Santa Fe, New Mexico, USA, May 29-June 2, 2011
PHONONICS-2011-0111

Acoustic phonon relaxation rates in nanometer-scale membranes

E. Chavez[1], P.O. Chapuis[2], J. Cuffe[2], F. Alzina[2], C.M. Sotomayor-Torres[2,3]
[1] *Dept. of Physics, Universitat Autònoma de Barcelona and Catalan Institute of Nanotechnology CIN2(ICN-CSIC), Campus de la UAB, 08193 Bellaterra (Barcelona), Spain, emigdio.chavez@icn.cat*
[2] *Catalan Institute of Nanotechnology CIN2(ICN-CSIC), Campus de la UAB 08193 Bellaterra (Barcelona), Spain, p2n@icn.cat*
[3] *Catalan Institute for Research and Advanced Studies (ICREA) 08010 Barcelona, Spain*

Abstract: The elastic continuum model is applied to analyse the acoustic phonon modes for single and three-layer membranes. The dispersion relations are computed using a numerical approach and are compared with experimental and theoretical results. These values are used to compute the rate of relaxation, considering a three-phonon Umklapp process.

The electronic properties of free-standing membranes, nanowires and ultrathin films, which are the buildings block of the components for the future electronics devices and nano-electrical mechanical nanostructures, have been the subject of the extensive studies. On the contrary, their thermal properties have received comparatively less attention. The phonon dispersion relation and the phonon interaction in such nanostructures are expected to be significantly different from due to bulk due to the confinement effects.

Our approach to investigate the phonon dispersion in free-standing layers is based in the elastic continuum model in isotropic media. Within this model, the equation of the phonon displacement vector, "***u***", may be written as[1]:

$$\partial^2 u / \partial t^2 = c_t^2 \nabla^2 u + (c_l^2 - c_t^2)\nabla(\nabla u) \tag{1}$$

where c_t and c_l are transversal and longitudinal sound speeds, respectively. The movement was solved for two different systems: (i) one layer of medium ***A*** of thickness ***a*** embedded in air, (ii) a stacking of three layers of alternating A and B media (see figure **1**).

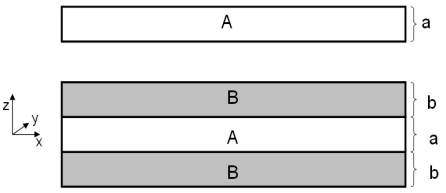

Figure 1 Structures considered for the present study

The general solution for the 1-layer system are: shear waves, dilatational (symmetric) and flexural (antisymmetric) waves[2]. The solutions for the 3-layer structures are: shear waves (only nonzero *y* components), symmetric *x* component and antisymmetric z component (SA waves), and antisymmetric x component and symmetric z component. The SA (AS) waves consists of dilatational (flexural) waves in the "***A***" layer and a linear combination of all waves in the two "***B***" layers. The calculated dispersion relations for flexural and SA waves are shown in the fig. **2** for a monolayer of silicon and the 3-layers structure SiO_2-Si- SiO_2. Note that the native oxide layers are in principle always present. Once obtained the dispersion relation we can derivate the group and phase velocity as well as the density of states.

From the first-order perturbation theory, the single-mode relaxation rate of Umklapp process (U) for a thermal mode $\boldsymbol{q}$ can written be as[3]:

$$\tau_U^{-1} = \sum_q \frac{8\gamma^2\hbar}{3\rho v^2}\omega_i\omega_j(\omega_i+\omega_j)\pi\delta[\Delta\omega][n(\omega_i)-n(\omega_i+\omega_j)] \tag{2}$$

where $\boldsymbol{\gamma}$ is the Grüneisen parameter, $\boldsymbol{v}$ is the sound velocity, $\boldsymbol{n(\omega_i)}$, $\boldsymbol{n(\omega_i+\omega_j)}$ are the equilibrium occupation of the states of $\boldsymbol{q_i}$, $\boldsymbol{q_i+q_j}$ and $\boldsymbol{\rho}$ is the density.

Phononics 2011: First International Conference on Phononic Crystals, Metamaterials and Optomechanics
Santa Fe, New Mexico, USA, May 29-June 2, 2011
PHONONICS-2011-0111

We calculate the different relaxation rates without approximation and compare our results with ref. **4**. We find a significant modification of the U-process in comparison to the case of bulk medium. Our aim is in particular to identify the implications of the presence of native oxide on the dispersion curves and the relaxation rates.

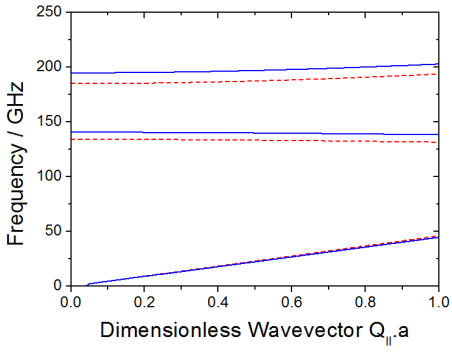

Figure 2: Dispersion curves of the flexural modes of a 30 nm Si membrane, (blue solid line) and 28.4nm Si with 1.6 nm SiO_2 on the top and bottom surfaces (red dashed line).

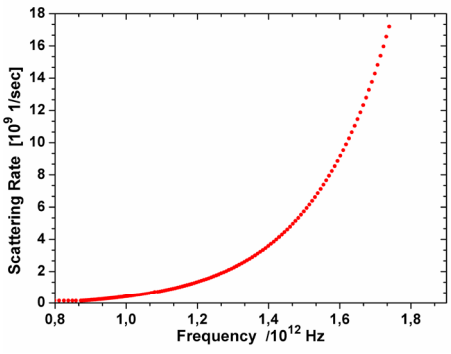

Figure 3: Phonon relaxation rates due to Umklapp process at T=300 K

References

[1] N. Bannov, V. Aristov, V. Mitin and M.A. Stroscio, *Phys. Rev. B*, **51**, 9930(1995).
[2] L. Donetti, F. Gámiz, J.B. Roldán and A. Godoy, *J. Appl. Phys.*, **100**, 013701 (2006).
[3] Y. Chen, D. Li, J.R. Lukes and A. Majumdar, *J. Heat Transf.*, **127**, 1129 (2005)
[4] A. Balandin and K.L. Wang, *Phys. Rev. B*, **58**, 1544(1998)

Phononics 2011: First International Conference on Phononic Crystals, Metamaterials and Optomechanics
Santa Fe, New Mexico, USA, May 29-June 2, 2011
PHONONICS-2011-0133

Nanoscale Phonon Engineering: From Quantum Dots and Nanowires to Graphene and Topological Insulators

Alexander A. Balandin

Department of Electrical Engineering and Materials Science and Engineering Program, Bourns College of Engineering, University of California – Riverside, Riverside, California 92521 U.S.A.
E-mail address: balandin@ee.ucr.edu

Abstract: I describe the nanoscale phonon engineering concept and its possible applications. Nanostructures offer new ways for controlling phonon transport via tuning phonon dispersion. Engineering the phonon spectrum can become as powerful a technique as the electron band-gap engineering, which revolutionized electronics. I outline recent examples of phonon engineering in quantum dot superlattices, nanowires, graphene ribbons and topological insulators. Particular attention is given to the phonon thermal transport in graphene and graphene's applications in thermal management.

The *nanoscale phonon engineering* is defined as controlled modification of the phonon spectrum and phonon transport in nanostructures with the goal of achieving higher electron mobility or changed thermal conductivity or other property, allowing for performance enhancement of electronic, thermoelectric or optoelectronic devices. The phonon engineering concept was initially introduced for nanostructures and nanodevices made of conventional semiconductors [1]. Tuning of the acoustic phonon spectrum in nanostructures with the acoustic impedance mismatch can help in achieving enhanced functionality such as decreased phonon thermal conductivity, beneficial for thermoelectric applications [2], or increased electron mobility [3]. The nanometer length scale, which is comparable to the thermal phonon wavelength in semiconductors, is essential for the phonon confinement effects and phonon engineering near room temperature (RT).

The change in the thermal conductivity of semiconductors due to the phonon – boundary scattering and phonon confinement effects bares important consequences for electronic industry in a view of continuous miniaturization. Heat in technologically important semiconductors is mostly carried by acoustic phonons. The feature size of the state-of-the-art transistor is already well below the RT phonon mean-free path (MFP) in Si, which is ~50 nm according to Debye model. In nanostructures with feature size W much smaller than the phonon MFP, the acoustic phonon spectrum undergoes modification and appears quantized provided that the structures are free standing or embedded within material with different elastic properties (acoustic impedance). This modification is particularly strong when W approaches the scale of the dominant phonon wavelength $\lambda \approx 1.48 \upsilon_S \hbar / k_B T$. Here k_B is the Boltzmann constant, T is the absolute temperature, $\hbar$ is the Plank's constant, and υ_S is the sound velocity. For many crystalline solids, λ is on the order of ~1.5 – 2 nm at RT, which is comparable to the thickness of the transistor gate dielectric or period of superlattices used in optoelectronic or thermoelectric devices.

The newly developed synthesis techniques have expanded the list of nanostructures and materials suitable for engineering the phonon spectrum. The "graphene revolution" started by the mechanical exfoliation of the single atomic layer graphene (SLG) made possible investigation of phonons in strictly two-dimensional (2D) systems. The knowledge about optical phonons in graphene led to the development of Raman spectroscopy as nanometrology tool for graphene identification on variable substrates and at different temperatures [4]. We have discovered experimentally that suspended graphene reveals an unusually high intrinsic thermal conductivity exceeding that of carbon nanotubes [5]. In order to measure the thermal conductivity of "free" graphene we developed on original optical non-contact technique (see Figure 1). The fact that the phonon thermal conductivity of large enough graphene flakes should be higher than that of the basal planes of bulk graphite was predicted theoretically by Klemens a decade ago. He pointed out at the fundamental differences in the long-wavelength phonon transport in 2D graphene and 3D graphite. Unlike in bulk graphite, in SLG the phonon transport remains 2D down to zero phonon energy, which results in larger contributions of long-wavelength

Phononics 2011: First International Conference on Phononic Crystals, Metamaterials and Optomechanics
Santa Fe, New Mexico, USA, May 29-June 2, 2011
PHONONICS-2011-0133

phonons to heat conduction [6]. It is also related to the fact that the intrinsic thermal conductivity in 2-D anharmonic crystals manifests divergence with the size of the system [7]. We were able to study the dimensional crossover of phonon transport both theoretically and experimentally using suspended few-layer graphene (FLG) flakes [7]. It was found that the "intrinsic" thermal conductivity of FLG reveals completely opposite dependence (see Figure 1) on the number of atomic planes (thickness) than the extrinsic thermal conductivity in conventional thin films, which is dominated by the phonon – boundary scattering. The extremely high thermal conductivity of graphene coupled with its flat geometry and demonstrated ability for functioning in Si-based devices make graphene promising material for engineering heat fluxes and thermal management of nanoelectronic circuits [8]. We extended the "graphene-like" mechanical exfoliation and phonon engineering techniques to other materials such as bismuth telluride, which are used for thermoelectric and topological insulator applications [9]. The knowledge of optical phonons allowed us to use Raman spectroscopy as nanometrology tool for topological insulators [10]. A detail review of the nanoscale phonon engineering in quantum dot superlattices, heterostructures and nanowires with acoustically mismatched barriers can be found in Ref. [11].

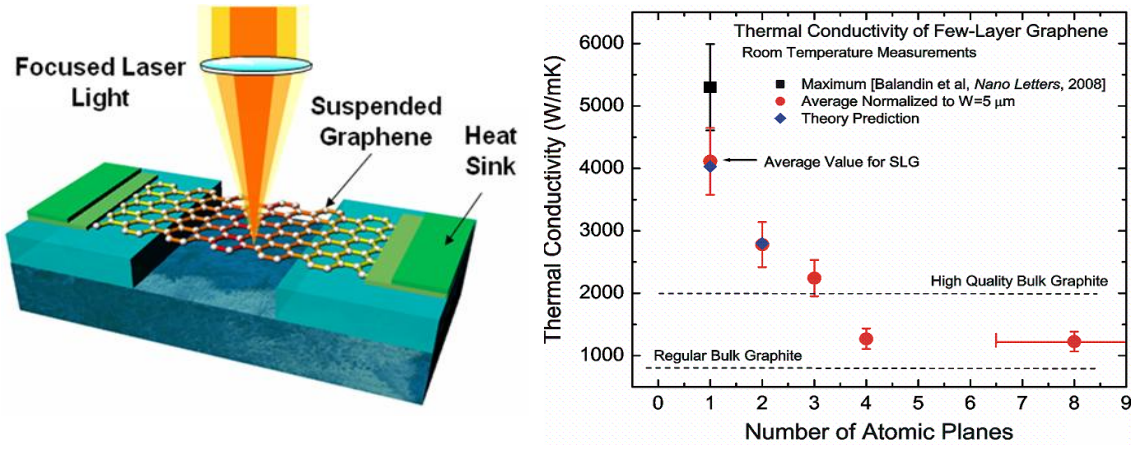

Figure 1 (Left panel) Schematic of the experimental set up, which was used for the first measurement of the thermal conductivity of graphene. In this experiment the excitation laser light focused on graphene suspended across a trench in Si wafer. Laser power absorbed in graphene induces a local hot spot and generates heat wave propagating toward the heat sinks. The local temperature rise was determined from the G peak shift in graphene Raman spectrum. (Right panel) The evolution of the phonon transport as system dimensionality changes from 2-D graphene to 3-D graphite revealed using suspended few-layer graphene samples. The figure is after Ref. [7].

This work was supported, in part, by AFOSR grant on Phonon Engineering, ONR grant on Graphene Quilts and SRC – DARPA Focus Center Research Program (FCRP) through its Functional Engineered Nano Architectonics (FENA) center.

References

[1] A. Balandin and K.L. Wang, *Phys. Rev. B*, **58**, 1544 (1998).
[2] J. Zou and A. Balandin, *J. Appl. Phys*., **89**, 2932 (2001).
[3] V.A. Fonoberov and A.A. Balandin, *Nano Letters*, **6**, 2442 (2006); D.L. Nika, et al., *Appl. Phys. Lett.*, **93**, 173111 (2008).
[4] I. Calizo, et al., *Nano Letters*, **7**, 2645 (2007); I. Calizo, et al., *Appl. Phys. Lett*., **91**, 201904 (2007).
[5] A.A. Balandin, et al., *Nano Letters*, **8**, 902 (2008); S. Ghosh, et al., *Appl. Phys. Lett*., **92**, 151911 (2008).
[6] D.L. Nika, et al., *Appl. Phys. Lett*., **94**, 203103 (2009); D.L. Nika, et al., *Phys. Rev. B*, **79**, 155413 (2009).
[7] S. Ghosh, D.L. Nika, W. Bao, S. Subrina, E.P. Pokatilov, C.N. Lau and A.A. Balandin, *Nature Materials,* **9**, 555 (2010).
[8] A.A. Balandin, *IEEE Spectrum*, 29, October (2009); S. Subrina, et al., *IEEE Electron Device Lett*., **30**, 1281(2009).
[9] D. Teweldebrhan, et al., *Nano Letters* (2010); D. Teweldebrhan, et al., *Appl. Phys. Lett*., **96**, 053107 (2010).
[10] K.M.F. Shahil, M.Z. Hossain, D. Teweldebrhan and A.A. Balandin, *Appl. Phys. Lett*., **96**, 153103 (2010).
[11] A.A. Balandin, *J. Nanoscience Nanotech*., **5**, 7 (2005); A.A. Balandin, E.P. Pokatilov and D.L. Nika, *J. Nanoelectron. Optoelectron*, **2**, 140 (2007).

Phononics 2011: First International Conference on Phononic Crystals, Metamaterials and Optomechanics
Santa Fe, New Mexico, USA, May 29-June 2, 2011
PHONONICS-2011-0145

Improved Lattice-Bath Phonon Relaxation in Nanoscale Oxides

Michael W. Blair[1], Bryan L. Bennett[1], Stephanie C. Tornga[1], Nickolaus A. Smith[1], Ross E. Muenchausen[1]

[1] *Materials Science and Technology, Los Alamos National Laboratory, P. O. Box 1663, MS E546, Los Alamos, NM, 87545, USA*
mblair@lanl.gov, blbennett@lanl.gov, sitarz@lanl.gov, nsmith@lanl.gov, rossm@lanl.gov

Abstract: Electron paramagnetic resonance (EPR) spectroscopy has been used to study energy transport properties of bulk and nanophosphor oxyorthosilicate samples. The bulk samples displayed a slight phonon bottleneck while energy relaxation in the nanophosphor samples was not influenced by the lattice-bath relaxation time and was more rapid.

Introduction

The scintillation properties of oxyorthosilicate materials doped with Ce such as Lu_2SiO_5 (LSO), Y_2SiO_5 (YSO), and Gd_2SiO_5 (GSO) have been studied extensively[1]. These materials are of particular interest for gamma ray detection as they have a high effective atomic number, high light output, fast decay times, and emit in the blue region which is advantageous for most detection systems.

LSO[2] and YSO[3] have also been studied by Electron Paramagnetic Resonance (EPR) spectroscopy in order to study the coordination environment of the Ce^{3+} sites. These studies determined that Ce replaces Lu or Y in the phosphors and occupies two different crystallographic sites corresponding to the two sites for Lu or Y. In previous papers[4] we have reported on EPR spectra of Ce^{3+} in both bulk and nanophosphor LSO and YSO and noted evidence of an increased disorder in the nanophosphor samples. However, the previous analysis used the simplified model of Pidol *et al.*[2], but, as will be shown, the EPR linewidths and relaxation mechanisms are more complicated than previously assumed. The goal of this paper is to further explore the temperature-dependent relaxation lifetimes and mechanisms of LSO:Ce and YSO:Ce for both Czochralski grown (bulk) samples and SCS nanophosphors.

Results and Discussion

Due to lifetime broadening the Ce^{3+} resonances can only be detected below approximately 50 K[4], and only the lowest doublet is occupied at this temperature. Figure 1 shows the Ce g_z resonance for nanophosphor YSO doped with 1% Ce for various temperatures where an increase in linewidth with increasing temperatures is evident. Nanophosphor LSO doped with 1 % Ce shows a similar behavior.

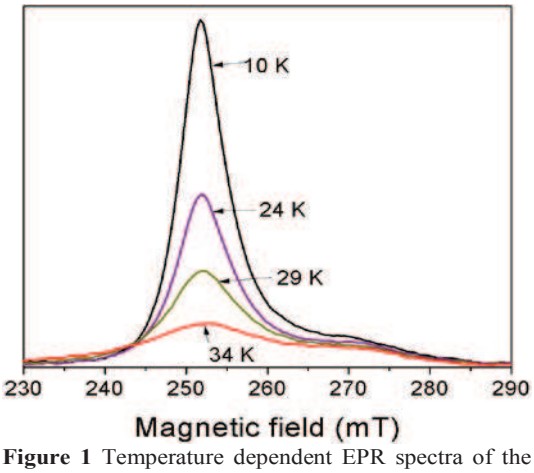

Figure 1 Temperature dependent EPR spectra of the Ce g_z resonance for SCS YSO with 1% Ce.

Although the increased linewidth with increasing temperature in Figure 1 is typical of an Orbach relaxation process, the analysis is complicated by the temperature-dependent lineshape of the samples. Pidol *et al.*[2] has previously noted that the EPR resonances of Ce-doped LSO were Gaussian at low temperatures and became progressively more Lorentzian with increasing temperatures, and our measurements follow the same pattern. In an attempt to separate these contributions to the overall lineshape, we fit the temperature-dependent EPR linewidths of Ce-doped YSO and LSO with a Voigt lineshape[5]. The results for the pure Lorentzian (w_L), pure Gaussian (w_g), and total (w_L+w_G) linewidths are shown in Figure 2 (a), (b), and (c), respectively.

The Lorentzian linewidths of Figure 2 (a) are related to the EPR relaxation lifetime τ by $\tau^{-1}=(2\pi g\beta L/h)$, and the lifetimes can be fit by a combination of a direct phonon relaxation process and the two phonon Orbach relaxation[6]:

Phononics 2011: First International Conference on Phononic Crystals, Metamaterials and Optomechanics
Santa Fe, New Mexico, USA, May 29-June 2, 2011
PHONONICS-2011-0145

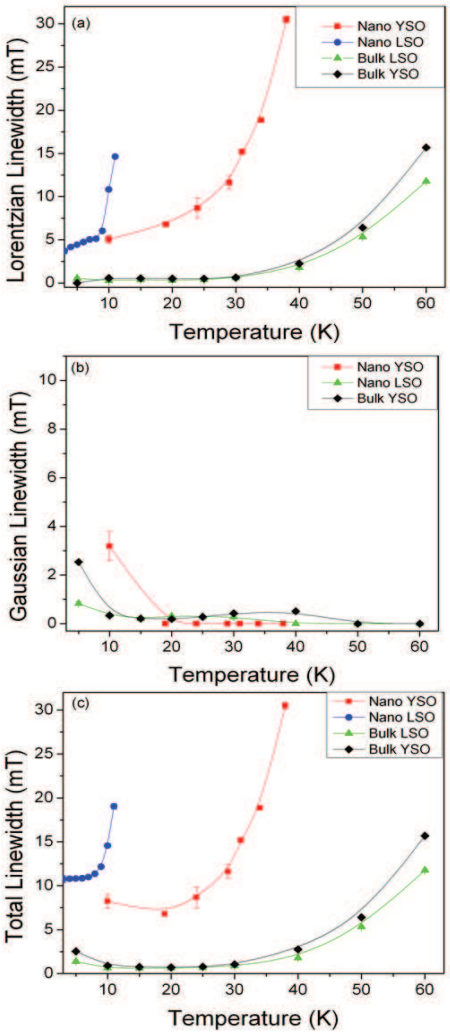

Figure 2 (a) Pure Lorentzian (wL), (b) pure Gaussian (wG), and (c) total (wL+wG) linewidths for bulk LSO, bulk YSO, nanophospor LSO, and nanophosphor YSO derived from fitting the Ce gZ resonance with a Voigt lineshape. The solid lines are guides for the eye only.

$$\frac{1}{\tau} = A*T^{n} + \frac{C*\Delta*^{3}}{\exp(\Delta E/k_B T) - 1)} \qquad (1)$$

where A is the direct phonon relaxation constant, k_B is Boltzmann's constant, T is the absolute temperature, C is the Orbach constant, and ΔE is the energy gap between the ground state of the Kramers doublet and the first excited state. In most cases n=1, but n=2 in the case of a phonon bottleneck where the heat transferred to the lattice cannot be effectively dissipated and the likelihood of phonon heating or energy transfer back to the spins is increased.

For bulk specimens, the temperature-dependent relaxation lifetimes could be fit with n=2 in Equation 1 and show a slight phonon bottleneck where the lifetime due to lattice-bath relaxation is comparable to the lifetime due to spin-lattice relaxation. The relaxation lifetime for the nanophosphors, though, do not show a dependence on the lattice bath relaxation process.

Conclusions and Future Work

The temperature dependence of the Ce g_z resonances was studied for both bulk and 1 % Ce-doped nanophosphor samples. By separating the homogeneous and inhomogeneous parts of the linewidths through Voigt lineshape analaysis, we were able to fit the Lorentzian linewidths to phonon relaxation processes that involve direct phonon relaxation and the two-phonon Orbach process[6]. The bulk samples displayed a weak phonon bottleneck where the lifetime of the lattice-bath relaxation process is comparable to the spin-lattice relaxation lifetime. The nanophosphor oxyorthosilicates, on the other hand, did not show any evidence of a phonon bottleneck. Unfortunately, due to the large uncertainties involved in this study, the analysis cannot be more quantitative but can identify significant and interesting trends.

The current study suggests the possibility of studying the complicated phonon relaxation process and energy transport in more detail. Future work will involve identifying a system or systems to address the various aspects of the phonon relaxation process. The ideal systems would allow for crystallite size and paramagnetic species concentration control at both the bulk (> 1 μm) and nanoscale. In addition, a symmetric crystal structure (e.g., cubic or hexagonal) that is invariant with reduced dimensionality, has well characterized sites for paramagnetic ions, and yields Lorentzian lineshapes would be preferred. Rare earth doped oxide crystals such as YAG:Ce or Y_2O_3:Tb may be suitable systems and are readily obtainable.

References

[1] R. Lecomte, C. Pepin, D. Rouleau, A. Saoudi, M.S. Andreaco, M. Casey, R. Nutt, H. Dautet, and P.P. Webb, *IEE Nucl. Sci. Symp.* **1,** 212 (1997).
[2] L. Pidol, O. Guillot-Noël, A. Kahn-Harari, B. Viana, D. Pelenc, and D. Gourier, *J. Phys. Chem. Solids* **67,** 643 (2006).
[3] I.N. Kurkin, K.P. Chernov, *Physica B & C* **101B+C,** 233 (1980).
[4] D.W. Cooke, M.W. Blair, J.F. Smith, B.L. Bennett, L.G. Jacobsohn, E.A. McKigney, and R.E. Muenchausen, *ITNS* **55,** 1118 (2008).
[5] A. Cabral-Prieto, H. Jiménez-Domínguez, L. González-Tovany, S. Galindo, H. Flores-Llamas, and M. Torres-Valderrama, *JMagR* **89,** 568 (1990).
[6] A. Abragam, B. Bleaney, *Electron Paramagnetic Resonance of Transition Ions*. Oxford University Press, London (1970).

Phononics 2011: First International Conference on Phononic Crystals, Metamaterials and Optomechanics

Santa Fe, New Mexico, USA, May 29-June 2, 2011

PHONONICS-2011-0156

Understanding and Controlling High-Frequency Phonon Thermal Energy Transport in Nanostructures

M. Maldovan[1]

[1] *Department of Materials Science and Engineering, Massachusetts Institute of Technology, 77 Massachusetts Av., Cambridge, MA 02139USA*
maldovan@mit.edu

Abstract: We present a novel theoretical approach based on the kinetic theory of transport processes to understand and accurately describe the transport of high-frequency phonon thermal energy in nanostructures over a broad range of temperatures and across multiple length scales, i.e. from nano to micro. Good agreement with experiments is obtained.

Modern experimental technologies enable the fabrication of complex nanostructures such as nanofilms, multilayers, superlattices, nanowires and nanotubes, nanoparticle composites, quantum dots, micro and nanoelectronic devices and MEMS. In many of the applications for which these nanomaterials are designed, the control of phonon heat transport is critical for the resultant energy efficiency of the device.[1-8] For example, materials with high thermal conductivities are necessary to rapidly dissipate heat in increasingly dense electronic devices such as computer microprocessors or semiconductor lasers. On the other hand, materials with low thermal conductivities are needed to increase the efficiency of energy conversion materials such as thermoelectrics (which can convert waste heat into electricity) or to create highly efficient thermal insulators (which can increase building energy efficiency for heating and cooling). The understanding and controlling of high-frequency phonon energy transport in nanostructured materials is thus crucial for the development of the new generation of energy efficient nanoscale devices in science and technology.

Thermal transport in solids is not necessarily a fixed material property but it can be controlled by modifying the thermal properties of phonons through different methods (e.g. impurities, lattice defects, geometry, etc.). Although the physical mechanisms governing the thermal conductivity of solids have been understood for years, a comprehensive theoretical method to accurately calculate the transfer of thermal energy, particularly at small scales, has not been available. This is due to the physical and mathematical complexity of three-phonon anharmonic processes and the effects of phonon scattering at the boundaries. At normal temperatures, phonon mean free paths are much smaller than the dimensions of macroscopic materials and the thermal conductivity is independent of material size and shape. As the material size is decreased, however, the thermal conductivity is reduced below that of the bulk material. This effect is mainly assigned to the shortening of the phonon mean free paths by collisions with the boundaries. One of the main difficulties of current theoretical models is to accurately calculate and predict this surface related reduction of the phonon mean free paths.

In this talk, we present a novel theoretical approach to understand and accurately describe the transport of phonon thermal energy in nanostructures over a broad range of temperatures and across multiple length scales, i.e. from nano to micro. The theoretical model is based on the kinetic theory of transport processes and includes the directional and spatial dependence for the reduction of the phonon mean free paths due to surface scattering. The model also considers general expressions for *all* physical variables involved in the transport of thermal energy such as dispersion relations $\omega_j(\mathbf{k})$, bulk phonon mean free paths $\ell_0(\mathbf{k})$, and surface specularity parameters $p(\mathbf{k})$. The thermal conductivity is calculated by using the formula

$$\kappa = \frac{1}{(2\pi)^3}\sum_j \int k_B(\hbar\omega_j/k_BT)^2 \frac{\exp(\hbar\omega_j/k_BT)}{[\exp(\hbar\omega_j/k_BT)-1]^2}\ \nu_j(\mathbf{k})\cos\theta\ \ell_j(\mathbf{k})\cos\theta\ d\mathbf{k} \qquad (1)$$

Phononics 2011: First International Conference on Phononic Crystals, Metamaterials and Optomechanics

Santa Fe, New Mexico, USA, May 29-June 2, 2011

PHONONICS-2011-0156

where $\hbar$ and k_B are the Planck and Boltzmann constants respectively, T is the temperature, $\omega_j = \omega_j(\mathbf{k})$ is the phonon frequency, $v_j(\mathbf{k}) = \nabla_{\mathbf{k}} \omega_j(\mathbf{k})$ is the group velocity, j refers to the different polarizations, and θ is the angle between the wavevector $\mathbf{k}$ and the thermal gradient ∇T.

We successfully applied the proposed theoretical model describing nanoscale heat transport to calculate the thermal conductivity of nanostructures (e.g. thin films, layered materials, nanowires, etc.). We obtained good agreement between our theoretical calculations and experimental measurements across different nanostructures, length scales, and temperatures. The final goal of this project is to be able to design, develop, and fabricate novel materials with specific (low or high) thermal conductivities and to create energy efficient microelectronic and optoelectronic devices and to increase the efficiency of many energy saving devices such as thermoelectrics and thermal insulators.

References

[1] D. G. Cahill *et al.* J. Appl. Phys. **93**, 793 (2003).
[2] A. I. Hochbaum *et al*., Nature **451**, 163 (2008).
[3] A. Boukai *et al*., Nature **451**, 168 (2008).
[4] R.M. Costescu *et al*., Science **303**, 989 (2004).
[5] C. Chiritescu *et al.*, Science **315**, 351 (2007).
[6] K. F. Hsu, *et al*., Science **303**, 818 (2004).
[7] B. Poudel, *et al*. Science **320**, 634 (2008).
[8] R. Venkatasubranian, E. Siivola, T. Colpitts, and B. O'Quinn. *Nature,* **413**, 597 (2001).

Phononics 2011: First International Conference on Phononic Crystals, Metamaterials and Optomechanics
Santa Fe, New Mexico, USA, May 29-June 2, 2011
PHONONICS-2011-0158

Nanophononics using Acoustic and Optical Cavities

N. D. Lanzillotti-Kimura[1,2], A. Fainstein[1], B. Jusserand[3], B. Perrin[3], A. Lemaitre[4], D. G. Schlom[5], A. Soukiassian[5]

[1] Centro Atómico Bariloche & Instituto Balseiro, C.N.E.A., R8402 AGP S. C. De Bariloche, Río Negro, Argentina
kimura@cab.cnea.gov.ar, afains@cab.cnea.gov.ar
[2] University of California – Berkeley, CA 94720, USA
[3] Institut des NanoSciences de Paris, CNRS – Université Pierre et Marie Curie, 75004 Paris, France
bernard.jusserand@insp.jussieu.fr, bernard.perrin@insp.jussieu.fr
[4] Laboratoire de Photonique et des Nanostructures, C.N.R.S., Route de Nozay, 91460 Marcoussis, France aristide.lemaitre@lpn.cnrs.fr
[5]Department of Materials Science and Engineering, Cornell University, Ithaca, New York, 14853-1501, USA
ds636@cornell.edu, soukiassian@gmail.com

Abstract: We report pump-probe time experiments in acoustic and optical cavities. We demonstrate that the generated coherent acoustic phonon spectra can be inhibited or enhanced in the cavity. Simulations highlight the role of the phonon density of states in the coherent phonon generation, extending concepts at the base of the Purcell effect to the field of phononics.

Changing the spontaneous light emission rate and spectra of atoms or excitons through the modification of the photon density of states has been the subject of significant efforts following Purcell's proposal and demonstration in the microwave domain.[1] This has been accomplished either by changing the dielectric boundaries close to the emitting species, or more fundamentally by embedding the emitter in an optical microcavity.[2] Depending on the tuning of the emitter spectra with maxima or minima of the modified photonic density of states, the emission can be either enhanced or inhibited. Similar ideas have been applied to modify other light-matter interactions processes. The search for large Purcell effects is at the heart of the quest for thresholdless lasing. In the field of phononics, and specifically the search of phonon lasing for efficient monochromatic THz sources, and for the control of heat at the nanoscale, these ideas have not been pursued to date. Here we demonstrate that the coherent acoustic phonon emission spectra of an impulsively excited thin metallic film can be either inhibited or enhanced by embedding the metal layer in an acoustic nanocavity.[3-6] This has been accomplished by using for the first time a hybrid metal cavity with $BaTiO_3/SrTiO_3$ epitaxial oxide phonon mirrors.

Acoustic nanocavities are the hypersound analog of the extensively studied optical microcavities.[3-6] We use a femtosecond laser light impulsion to generate a pulse of coherent sub-THz phonons in a metallic layer, and then we study how the latter is modified by changing the structure around the metal film. We compared two samples, in the first one we deposited the Ni film directly on a $SrTiO_3$ substrate, while in the second one the film is embedded in an acoustic nanocavity. In the latter, we chose as bottom broadband acoustic mirror $BaTiO_3/SrTiO_3$ superlattice (SL) grown by molecular beam epitaxy on a $SrTiO_3$ substrate. $BaTiO_3$ and $SrTiO_3$ have optical energy gaps in the 350 nm range and are consequently completely transparent at the laser energy of 750 nm. In this way, the acoustic mirrors only affect the acoustic boundary conditions of the metallic film, and thus its local acoustic density of states. The sample-air interface responds to a free surface boundary condition. This surface performs as the top mirror to complete the phonon cavity. Both the coherent phonon generation and detection are performed only at the metallic films. In the case of the acoustic nanocavity the measured spectrum presents an enhanced peak at the confined mode energy, while in the case of the naked Ni film the spectrum is broad and featureless. Moreover, we observed the inhibition of the coherent phonon emission in the region of the acoustic stop-band. In other words, within the phononic stop-band modes are expelled and they concentrate at the cavity resonance and at the stop-band edges. It is this modification of the mode density landscape that determines at which energies acoustic phonons can be emitted by the metallic layer (enhancement at the cavity mode), and at which they cannot (inhibition within the phonon gap). In addition, outside the phononic stop-band oscillations develop in the generated spectrum which, when compared with the bare Ni-film, also express weaker but clear inhibition and enhancement regions. The experiments are compared with calculations of the impulsive

Phononics 2011: First International Conference on Phononic Crystals, Metamaterials and Optomechanics
Santa Fe, New Mexico, USA, May 29-June 2, 2011
PHONONICS-2011-0158

generation and detection of coherent phonons that highlight the role of the phonon density of states on the acoustic emission rate, extending the concept of the optical Purcell effect to the field of phononics.

In addition, we report experiments performed on structures based in semiconductor optical microcavities, where acoustic phonons and photons can be confined simultaneously. Thus, both the optical and acoustic densities of states result modified.[7-8] An optical microcavity confines the electromagnetic field both spectrally and spatially, inducing strong changes in the light-matter interaction and giving rise to novel physical phenomena and devices. In the case of planar semiconductor optical microcavities, two distributed Bragg reflectors (DBRs) enclose an optical spacer. The confinement characteristics and the amplification of the electric field are determined by the selection of materials, thickness, and number of periods that constitute each DBR and the optical spacer. Optical microcavities have been the subject of very active research during the last 15 years, and have been used to study the modification of the photonic lifetimes, parametric oscillations, cavity polariton Bose-Einstein condensates, the polariton laser, and amplification of Raman scattering signals, among others.[9-11]

Particularly, the photonic confinement and amplification have been used in these high-Q resonators to amplify the optical generation of incoherent phonons through Raman processes and to evidence new effects in the phonon physics and dynamics in semiconductor nanostructures. This scheme was used to study confined phonons in acoustic nanocavities. The optical resonances can be complemented with electronic resonances giving rise to amplified Raman cross-sections of up to 10^7. On the contrary, the use of optical confinement for the enhanced coherent generation of acoustic phonons (in contrast with incoherent generation by spontaneous Raman scattering) is a concept that has been little treated up to now. The realization of a monochromatic, coherent, and intense source of ultrahigh frequency acoustic phonons based on semiconductor optical microcavities and the obtained coherent phonon enhancements will be also discussed.

References

[1] E. Purcell, in Proceedings of the American Physical Society, 1946 [Phys. Rev. **69**, 681 (1946)].
[2] E. Yablonovitch, Phys. Rev. Lett. **58**, 2059 (1987).
[3] M. Trigo, A. Fainstein, B. Jusserand, and V. Thierry-Mieg, *Phys. Rev. Lett.* **89**, 227402 (2002).
[4] A. Huynh, N. D. Lanzillotti-Kimura, B. Jusserand, B. Perrin, A. Fainstein, M. F. Pascual-Winter, E. Peronne, and A. Lemaître, Phys. Rev. Lett. **97**, 115502 (2006)
[5] N. D. Lanzillotti-Kimura, A. Fainstein, A. Huynh, B. Perrin, B. Jusserand, A. Miard, and A. Lemaître, *Phys. Rev. Lett.* **99**, 217405 (2007).
[6] A. Huynh, B. Perrin, N. D. Lanzillotti-Kimura, B. Jusserand, A. Fainstein, and A. Lemaître, Phys. Rev. B **78**, 233302 (2008)
[7] N. D. Lanzillotti-Kimura, A. Fainstein, B. Jusserand, and A. Lemaître, Phys. Rev. B **79**, 035404 (2009)
[8] N. D. Lanzillotti-Kimura, A. Fainstein, B. Perrin, B. Jusserand, A. Soukiassian, X. X. Xi, and D. G. Schlom, *Phys. Rev. Lett.* **104**, 187402 (2010).
[9] D. Sanvitto, F. M. Marchetti, M. H. Szymanska, G. Tosi, M. Baudisch, F. P. Laussy, D. N. Krizhanovskii, M. S. Skolnick, L. Marrucci, A. Lemaître, J. Bloch, C. Tejedor, and L. Vina, Nature Physics **6**, 527 (2010)
[10] E. Wertz, L. Ferrier, D. D. Solnyshkov, R. Johne, D. Sanvitto, A. Lemaître, I. Sagnes, R. Grousson, A. V. Kavokin, P. Senellart, G. Malpuech and J. Bloch, Nature Physics **6**, 860 (2010)
[11] A. Fainstein and B. Jusserand, Light scattering in Solids IX: Novel Materials and Techniques 108, 17, (Springer, Heidelberg, (2007)

Phononics 2011: First International Conference on Phononic Crystals, Metamaterials and Optomechanics
Santa Fe, New Mexico, USA, May 29-June 2, 2011
PHONONICS-2011-0174

Reduction of Thermal Conductivity in Silicon Slabs by Unit Cell Nanostructuring

Bruce L. Davis, Mahmoud I. Hussein

Department of Aerospace Engineering Sciences, University of Colorado at Boulder, Boulder, CO 80309, USA
bruce.davis@colorado.edu, mih@colorado.edu

Abstract: The emerging field of *phononics* is enabling a cross-flow of ideas pertaining to wave propagation in periodic media to be transferred from one scale to another. Just like unit cell structuring has seen much interest in phononic crystals for the control of sound and vibration, the same can be done at the nanoscale for the control of thermal properties. Here we present ideas for *unit cell nanostructuring* within thin silicon slabs for the purpose of reducing the thermal conductivity. To assess our models we use a Callaway-Holland-type scheme for the thermal conductivity prediction, and employ full-fledged lattice dynamics calculations to accurately capture the dispersion of the nanostructured silicon slabs.

The phonon band structure of a crystalline solid has a direct influence on its thermal conductivity, especially at conditions where coherent transport is dominant. Key features of the band structure are frequency band gaps and the values of the group velocity at each dispersion branch. Beyond linear dispersion, other important quantities are the nature of the different types of nonlinear wave interactions (expressed in terms of scattering/relaxation times), the heat capacity, the presence of defects, and the ambient temperature. A strong understanding of the effects of these parameters will enable a new material design paradigm towards potentially dramatic reductions in the thermal conductivity. Many applications stand to benefit from such an advance, chief among them is the development of thermoelectric energy conversion materials with very high values of the figure-of-merit (a metric for quantifying the performance of the energy conversion).

The concept of phonon engineering of nanoscale structures has been a topic of intense research in recent years, e.g., Ref. 1. Among the various phonon engineering strategies considered is the idea of utilizing phononic crystals at the nanoscale to provide a means for a controlled influence on the phonon transport properties, e.g., Refs. 2-8. Among the configurations considered is the insertion of periodic holes in silicon slabs[6,7]. By selecting appropriately large dimensions for the lattice spacing and the holes diameter, phonons will destructively interfere and will nonlinearly scatter while minimal electron scattering will be incurred. In this manner the thermal conductivity can be reduced without altering the electronic properties (a favorable outcome for thermoelectric materials). A recent study based on a continuum model for the phononic crystal band structure has demonstrated this advantage[7]. A continuum model however over-simplifies the phonon band structure and does not capture the subtle characteristics of the higher-order optical modes. In this paper we carry out full-fledged lattice dynamics calculations on the silicon slab supercells with and without holes, and proceed to investigate the effects of the periodic holes on the thermal conductivity.

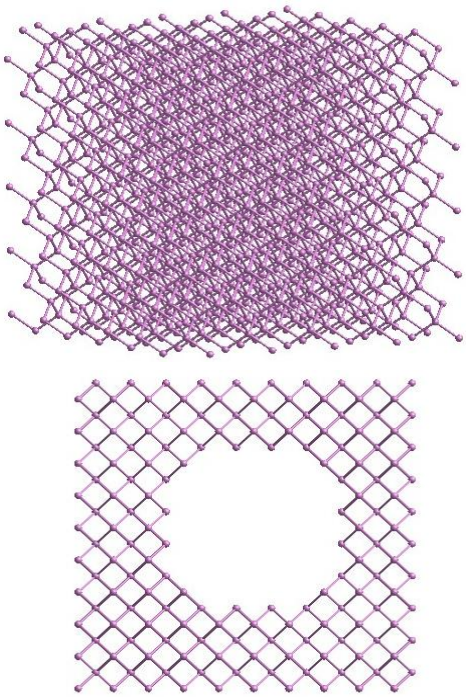

Figure 1: 5x5x5 Silicon slab (top) containing 1000 atoms. Silicon slab with periodic holes (bottom).

We consider silicon slabs formed by extending the diamond cubic 8-atom unit cell along the Cartesian directions. For the interatomic potential we utilize the Tersoff potential with second nearest neighbor interactions considered. The slab size analyzed is a 5x5x5 supercell measuring 2.7 nm along each Cartesian direction and contains 1000 atoms.

Phononics 2011: First International Conference on Phononic Crystals, Metamaterials and Optomechanics
Santa Fe, New Mexico, USA, May 29-June 2, 2011
PHONONICS-2011-0174

The hole diameter is set to be 0.6 of the lattice constant (Fig. 1). Given that the lattice dynamics formulation models the motion of each individual atom, limited computational resources prevent us from considering larger dimensions; however, this initial study provides a proof-of-concept. Prior to computing the band structure, surface relaxation along the top and bottom boundaries of the slab and around the holes is implemented. Fig. 2 (left) shows the band structure of this relaxed slab configuration compared to that of a bulk silicon supercell of the same size. Clearly, the acoustic branches exhibit slab-like properties with a reduced group velocity at low wave numbers. Upon introducing the periodic holes (Fig. 2, right), a flattening of the branches is observed within both the acoustical and optical modes in addition to a general reduction in frequencies. These band structure alterations have a significant effect on the thermal conductivity; using a Callaway-Holland-type scheme for thermal conductivity prediction, a minimum of 5% reduction is noted for the slab with periodic holes compared to the slab without the holes. This calculation was conducted for room temperature and only considered Umklapp scattering. We have neglected boundary scattering which is a conservative approximation because our interest is thermal conductivity reduction. Upon further refinement of our modeling parameters a higher reduction in thermal conductivity is expected as reported in Refs. 6,7. In future studies, we will consider nanostructuring the configuration of the supercell (see Ref. 4 for one-dimensional nanoscale phononic crystals) in order to obtain more profound changes to the band structure and consequently stronger reductions in the thermal conductivity.

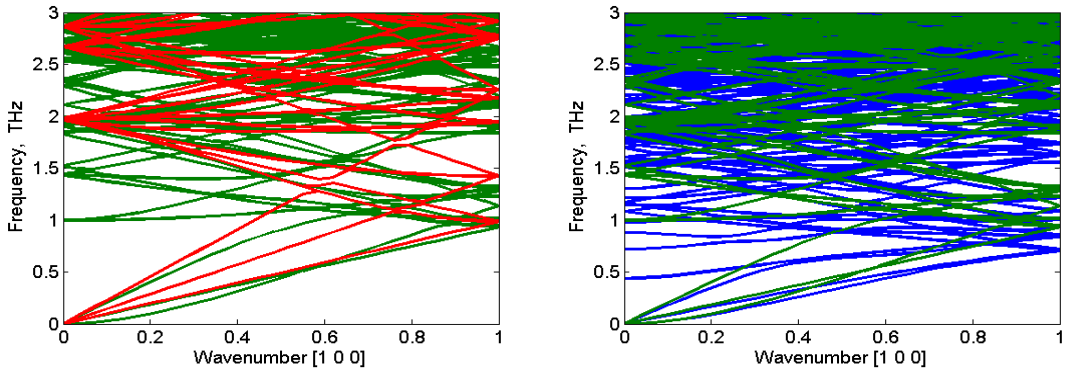

Figure 2: Silicon slab based on a 5x5x5 supercell (1000 atoms) with surface relaxation (green) compared with 5x5x5 bulk silicon (red) and a 5x5x5 slab with periodic holes (blue).

References

[1] A. A. Balandin, *J. Nanosci. Nanotechnol.* **5**, 1015 (2005).
[2] T. Gorishnyy, C. K. Ullal, M. Maldovan, G. Fytas, E. L. Thomas, *Physical Review Letters*, **94**, 115501 (2005).
[3] A. J. H. McGaughey, M. I. Hussein, E. S. Landry, M. Kaviany and G. M. Hulbert, *Physical Review B*, **74**, 104304 (2006).
[4] E. S. Landry, M. I. Hussein and A. J. H. McGaughey, *Physical Review B*, **77**, 184302 (2008).
[5] J.-N. Gillet, Y. Chalopin, and S. Volz, *Journal of Heat Transfer*, **131**, 043206 (2009).
[6] J. K. Yu, S. Mitrovic, D. Tham, J. Varghese and J. R. Heath, *Nature Nanotechnology*, **5**, pp. 718-721 (2010)
[7] P. E. Hopkins, C. M. Reinke, F. S. Mehmet, R. H. Olsson, E. A. Shaner, Z. C. Leseman, J. R. Serrano, L. M. Phinney, I. El-Kady, *Nano Letters* **11**, pp. 107–112 (2011).
[8] J. F. Robillard, K. Muralidharan, J. Bucay, P. A. Deymier, W. Beck and D. Barker, *Chinese Journal of Physics*, 49, pp. 448-461 (2011).
[9] J. Callaway, *Physical Review*, **113**,1046-1051 (1959).

Phononics 2011: First International Conference on Phononic Crystals, Metamaterials and Optomechanics
Santa Fe, New Mexico, USA, May 29-June 2, 2011
PHONONICS-2011-0176

Convergence of the Reduced Bloch Mode Expansion Method for Electronic Band Structure Calculations

Qiong. Guo, Osama. R. Bilal, Mahmoud. I. Hussein

Department of Aerospace Engineering Sciences, University of Colorado at Boulder, Boulder, USA
Qiong.Guo@colorado.edu, Osama.Bilal@colorado.edu, mih@colorado.edu

Abstract: Reduced Bloch mode expansion is a Bloch modal analysis method that enables exceptionally fast, yet accurate, periodic media band structure calculations. In this paper, the method is tested on electronic band structure calculations for a high-symmetry cubic model and a low-symmetry triclinic model, both based on the Kronig-Penney fixed potential. For both cases, the energy (eigenvalues) and wave functions (eigenvectors) demonstrate very good convergence performance.

Band structure calculations provide a basis for the study of thermal, optical and magnetic properties of crystals. Numerous techniques are available for band structure calculations. All techniques however suffer from the common problem that the computational load for solving the underlying complex eigenvalue problem over many **k**-points in the Brillouin zone is prohibitive. To expedite this process, there are several methods that aim to approximate the band structure between **k**-points[1]. We recently proposed a new method that enables such an approximation at an extremely low cost with negligible loss in accuracy. This method is referred to as the Reduced Bloch Mode Expansion (RBME) method[2]; it applies to both classical and *ab initio* band structure calculations of periodic media. Furthermore, the method is applicable to any type of wave propagation problem: phononic, photonic, electronic etc.

The RBME employs a natural basis composed of a selected reduced set of Bloch eigenfunctions. The displacement Bloch function $\tilde{u}$ is expressed as a superposition of an extremely small truncated set of m Bloch mode eigenfunctions $\tilde{v}$, thus enabling a linear transformation from the full-size problem to a set of reduced modal coordinates,

$$\tilde{u}(x) \cong \sum_{j=1}^{m} \beta_j \tilde{v}_j(x), \qquad m \in \text{integer}. \tag{1}$$

As RBME is practically a secondary expansion, we can use any of the common expansion methods to undergo a primary expansion of the periodic unit cell and solution field. In our work we use the finite element (FE) method. After discretization and application of Bloch theory to the governing equation of motion for the wave propagation problem we are considering, an eigenvalue problem emerges:

$$(A(k) - \lambda I)\tilde{U} = 0. \tag{2}$$

Solution of Eq. (2) at selected **k**-points provides the eigenvectors from which a reduced *Bloch modal matrix*, Ψ, is formed. This matrix is then used to linearly transform the problem:

$$\tilde{U}_{(n\times 1)} = \Psi_{(n\times m)} \tilde{V}_{(m\times 1)}, \quad m << n \tag{3}$$

Substituting Eq. (3) into Eq. (2), and pre-multiplying by the complex conjugate of Ψ yields a reduced eigenvalue problem of size $m \times m$:

$$(\overline{A}(\mathbf{k}) - \lambda I)\tilde{V} = 0, \quad \overline{A}(\mathbf{k}) = \Psi^* A(\mathbf{k}) \Psi. \tag{4}$$

Only if the reduced basis is suitably chosen can the proposed RBME approach produce accurate results. First, an appropriate choice of eigenfunctions in certain reference points in the **k**-space needs to be made. A "2-point expansion scheme" involves choosing eigenfunctions corresponding to the high symmetry points determined by the medium's crystal structure and group theory along the border of the IBZ. By augmenting with additional intermediate **k**-points centerally intersecting the straight lines joining the points chosen in the 2-point expansion scheme, a higher order expansion scheme is realized (Figure 1). Second, in order for the band structure calculations to be accurate up to the frequency (energy) range of interest, the number of eigenfunctions retained at each of the **k**-points selected should be slightly higher than the number of dispersion branches that are to be computed. Further resourceful utilization of the Bloch eigenfunctions is made by only using those eigenfunctions that correspond to a selection of **k**-points belonging to the current IBZ circuit line that is being evaluated; in this case the line is divided into "windows" for which only two sets of eigenfunctions are employed.

Phononics 2011: First International Conference on Phononic Crystals, Metamaterials and Optomechanics
Santa Fe, New Mexico, USA, May 29-June 2, 2011
PHONONICS-2011-0176

In this work we apply the RBME method to electronic band structure calculations for both cubic and triclinic lattices. Starting from the time-independent single electron Schrödinger equation, the three-dimensional generalized Kronig-Penney model is chosen for the electronic potential[3].

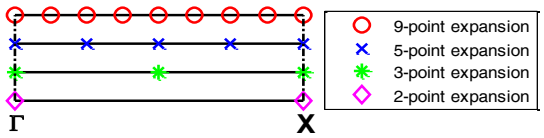

Figure 1 Illustration of four k-point selection schemes.

$$V(x)=\sum_{i=1}^{3}\bar{V}(x_i)\text{, where }\bar{V}(x_i)=\begin{cases}0, 0\le x_i<2a.u.,\\ 6.5Ry, 2a.u.\le x_i<3a.u.\end{cases} \quad (5)$$

The unit cell is discretized into 9×9×9 uniformly sized 8-node trilinear hexahedral finite elements, i.e. n_{el} =729. The **k**-space is discretized such that a total of 65 **k**-points are evaluated to generate the band structure. Figure 2 shows the electronic band structure containing the first 8 branches following the **k**-space paths $\Gamma\rightarrow$X$\rightarrow$M$\rightarrow$R$\rightarrow\Gamma$ for the cubic case (Figure 2.1), and B$\rightarrow\Gamma\rightarrow$F$\rightarrow\Gamma\rightarrow$G for the triclinic case[4] (Figure 2.4). The RBME results (based here on a 3-point expansion and use of eight Bloch modes for every selected **k**-point) provide an excellent approximation to the results of the full model, noting the reduction in the size of the matrix problem is from 729×729 to 24×24. The absolute error of eigenvalues $e_{eval}=E_{Full}-E_{RBME}$ for the cubic and triclinic cases (Figure 2.2 and 2.5) for the first three branches converges rapidly with the number of expansion points $n_{\exp}$. The rapid convergence of the maximum L^2 norm of the absolute error of eigenvectors for first 10 branches $e_{vect}=\sum_{i=1}^{10}\left|\tilde{U}_{Full,i}\right|^2-\sum_{i=1}^{10}\left|\tilde{U}_{RBME,i}\right|^2$ has also been computed (Figures 2.3 and 2.6); the order of maximum error is 1x10^{-3}.

$$V(x)=\sum_{i=1}^{3}\bar{V}(x_i)\text{,}\quad\text{where }\bar{V}(x_i)=\begin{cases}0, 0\le x_i<2a.u.,\\ 6.5Ry, 2a.u.\le x_i<3a.u.\end{cases} \quad (5)$$

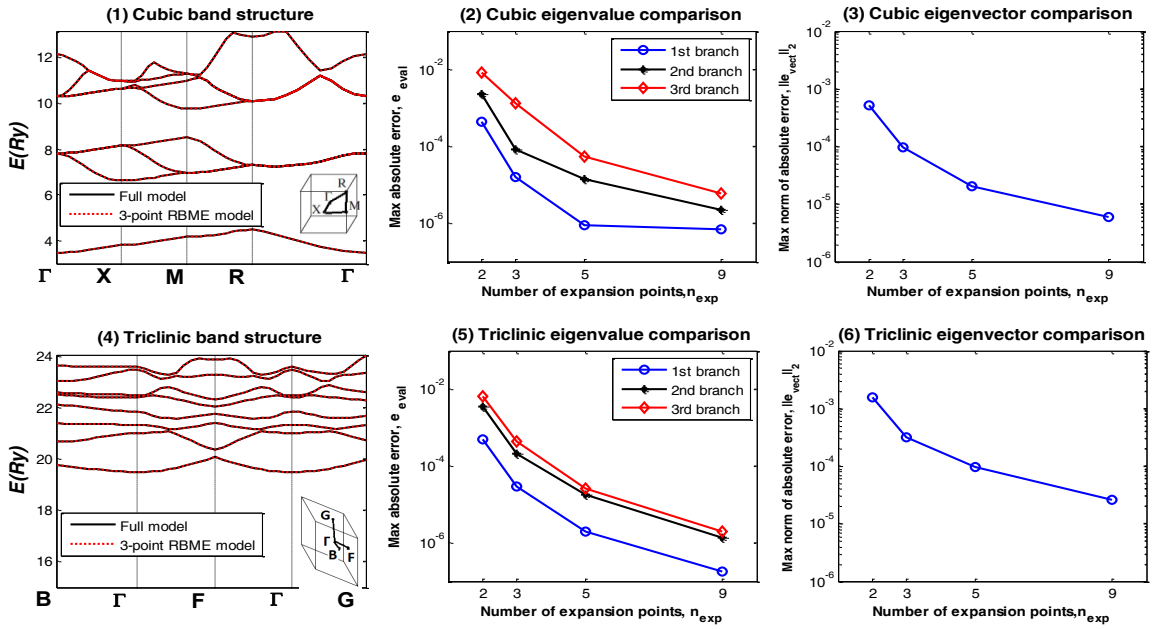

Figure 2 Performance of the RBME method in electronic band structure calculations. Band structure for the cubic (1) and triclinic (4) cases. Error of eigenvalues and eigenvectors for the cubic (2,3) and triclinic (5,6) cases.

References

[1] H. J. Monkhorst and J. D. Pack, *Phys. Rev. B* **13**, 5188-5192 (1976)
[2] M. I. Hussein, *Proc. R. Soc. A.* **465**, 2825-2848 (2009)
[3] J. E. Pask, B. M. Klein, P.A. Sterne, and C.Y. Fong, *Comp. Phys. Commun.* **135**, 1-34 (2001)
[4] T. Hahn, *International Tables for Crystallography*, *Vol. A*: Space Group Symmetry, Holland (1983)

Phononics 2011: First International Conference on Phononic Crystals, Metamaterials and Optomechanics
Santa Fe, New Mexico, USA, May 29-June 2, 2011
PHONONICS-2011-0183

Thermal Conductivity Reduction in Phononic Crystals: Interplay of Coherent versus Incoherent Scattering

Thomas E. Beechem[1], Patrick E. Hopkins[1], Charles M. Reinke[1], Mehmet F. Su[2], Bongsang Kim[1], Charles. T. Harris[1], Drew Goettler[2], Maryam Ziaei-Moayyed[1], Eric A. Shaner[1], Zayd C. Leseman[2], R. H. Olsson III[1], Alan McGaughey[3], I. El-Kady[1,2]

[1]Sandia National Laboratories, Albuquerque, NM, USA,
tebeech@sandia.gov, pehopki@sandia.gov, cmreink@sandia.gov, bonkim@sandia.gov, ctharri@sandia.gov, mziaeim@sandia.gov, eashane@sandia.gov, rholsso@sandia.gov, ielkady@sandia.gov
[2]University of New Mexico, Albuquerque, NM, USA
mfatihsu@.unm.edu, goettled@unm.edu, zleseman@unm.edu
[3]Carnegie Mellon University, Pittsburgh, PA, USA
mcgaughey@cmu.edu

Abstract: In this talk we pose the question: Can the coherent scattering events brought by the periodicity of the Phononic Crystal (PnC) lattice affect the high frequency THz phonons that dominate heat transfer process? In other words, can PnC patterning be used to manipulate the thermal conductivity of a material? We report both theoretically and experimentally on the role of coherent versus incoherent scattering of phonons by a 2D PnC structure and the efficacy of each process in both the cross-plane and in-plane directions of the PnC lattice.

Phonons propagating in a Phononic Crystal (PnC) lattice undergo two distinct types of scattering mechanisms: Coherent and incoherent scattering. Coherent scattering is brought about by Bragg scattering events which result primarily in the creation of phononic gaps where the propagation of phonons are prohibited, anomalous and flat, dispersionless bands, and negative phonon group velocities. The combination of these phenomena results in a rich complicated band structure (dispersion) compared to that of the bulk solid in absence of PnC structuring, accompanied by a redistribution of the phononic density of states (DOS). Incoherent boundary scattering, on the other hand, arises as a consequence of scattering due to the mechanical impedance mismatch between the host background matrix and the scattering centers, though the interference is not coherent. While coherent scattering phenomena have been readily validated to affect the low frequency (RF) phonons, in this communication we question the possibility of extending these effects to the high frequency THz phonons that dominate heat transfer process.

To answer this question we start by calculating the dispersion of a square PnC lattice of air holes in a Si matrix using the plane wave expansion technique. Here we draw on the fact that the longitudinal acoustic mode in silicon is linear up to ~10THz, while the transverse modes are linear up to ~3THz, thus allowing us to assume a homogenous "Ether" of Si where the average elastic properties are assumed up to 3THz. To predict the amount of thermal conductivity we expect resulting from phonon scattering by the Si/Air-PnC, we take a Callaway-Holland-type model[1]:

$$\kappa = \frac{1}{6\pi^2}\sum_j \int_q \frac{\hbar^2 \omega_j^2(q)}{k_B T^2} \frac{\exp\left[\frac{\hbar\omega_j(q)}{k_B T}\right]}{\left(\exp\left[\frac{\hbar\omega_j(q)}{k_B T}\right]-1\right)^2} v_j^2(q)\tau_j(q)q^2 dq \qquad (1)$$

where $\hbar$ is Planck's constant, $\omega(q)$ is the phonon dispersion, k_B is the Boltzmann constant, T is the phonon temperature, $v(q)=\partial\omega(q)/\partial q$ is the phonon group velocity, $\tau(q)$ is the scattering time of the phonons, q is the wavevector, and the thermal conductivity, κ is summed over all modes.

On the other hand, to investigate the effect of pure incoherent scattering by the PnC pores, lattice dynamics based calculations were performed using the Stillinger-Weber (SW) interatomic potential. Here our approach consists of combining bulk phonon properties with a boundary scattering model to predict the thermal conductivity of a nanostructure. Harmonic and anharmonic lattice dynamics calcu-

Phononics 2011: First International Conference on Phononic Crystals, Metamaterials and Optomechanics
Santa Fe, New Mexico, USA, May 29-June 2, 2011
PHONONICS-2011-0183

lations were performed to obtain the group velocity vectors ($\boldsymbol{v}_g$), and mean free paths (Λ_{bulk}) for 27,786 phonon modes (denoted by subscript i) uniformly distributed through the first Brillouin zone of bulk SW silicon. A geometric model of the PnC unit cell was created and a random point (denoted by subscript j) was randomly chosen within it. From this point, a line in the direction of the group velocity vector (the direction of energy transport) for each phonon mode is extended. The distance, d_{ij}, to the first intersection with a solid surface (the top or bottom of the film or the side of a hole) is calculated based purely on the geometry. This distance is combined with the bulk mean free path of that mode using the Matthiessen rule to obtain an effective mean free path for each mode from that starting point: $\frac{1}{\Lambda_{ij}} = \frac{1}{\Lambda_{i,bulk}} + \frac{1}{d_{ij}}$ The values of Λ_{ij} for each phonon mode are then averaged over 10,000 random points in the unit cell to give the effective mean free path of each phonon mode, Λ_i. Using the effecting mean free paths, the cross-plane thermal conductivities of the solid material in the PnC are calculated from a summation over all phonon modes as

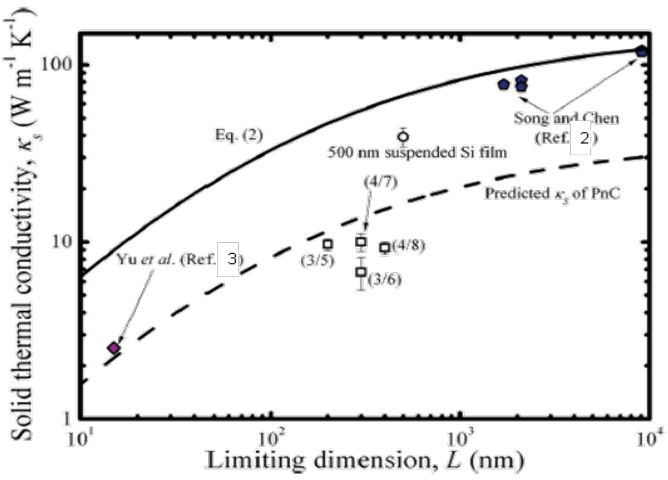

Figure 1.The measured thermal conductivity of Si structures at room temperature as a function of the minimum feature size L for the PnCs (unfilled squares)[1], microporous solids (filled pentagons),[2] nanomesh (filled diamond),[3] and a suspended 500 nm thick Si film – that is, an unpatterned Si slab (unfilled circle). The dashed line is the predictions of Eq. (1) using the PnC dispersion while the solid line corresponds to the predictions of Eq. (2) assuming only incoherent scattering.

$$\kappa_{PnC-Inconerent} = \sum_i c_{v,i} v^2{}_{g,i} \frac{\Lambda_i}{|v_{g,i}|} \tag{2}$$

where $c_{v,i}$ is the volumetric specific heat and $v_{g,i,}$ is the component of the group velocity vector in the cross-plane direction. To convert these solid thermal conductivities to values that can be compared to the experimental measurements, the porosity of the PnC is then factored in by multiplying with the factor $[(1+2\phi/3)/(1-\phi)]$, where φ is the porosity of the lattice.

The results of Eq. 1 and 2 are shown in Figure 1 as a function of the minimum feature size and is compared to measured the thermal conductivity of Si PnC plates using the time-domain thermoreflectance technique (TDTR)[1]. The results show a massive thermal conductivity reduction from 148W/mK for bulk silicon to 6.1W/mK for the Si-PnC; approximately 96% reduction. They further show that incoherent scattering over predicts the thermal conductivity of the PnC-lattice by more than a factor of 2, leading us to suspect that coherent scattering brought through by the PnC dispersion may be playing a significant role in this reduction. Similar calculations and measurements were also carried out in the in-plane direction and a discrepancy between the thermal conductivity reduction purely based on incoherent scattering effects, while not as pronounced, was also seen to be evident. In this talk we present a possible explanation for the difference between the in-plane and cross-plane results, as well as a possible theorization of the role of optical phonons in this process.

References

[1] P. E. Hopkins, C. M. Reinke, M. F. Su, R. H. O. III, E. A. Shaner, Z. C. Leseman, J. R. Serrano, L. M. Phinney, and I. El-Kady, *Nanoletters* **11**, 107-112, (2011).
[2] A. I. Hochbaum, R. Chen, R. D. Delgado, L. Wenjie, E. C. Garnett, M. Najarian, A. Majumdar, and Y. Peidong, , *Nature* **451**, 163-167, (2008).
[3] L. M. Ivanova, P. A. Aleksandrov, and K. D. Demakov, *Inorganic Materials* **42**,1205-1209, (2006).

Phononics 2011: First International Conference on Phononic Crystals, Metamaterials and Optomechanics
Santa Fe, New Mexico, USA, May 29-June 2, 2011
PHONONICS-2011-0185

Isotopically Enriched Semiconductor Superlattices for Thermoelectric Applications

A. Vogelsang[1], S. M. Ullah[1], G. Bastian[1], A. Plech[2], N. Wehmeier[3], H. Bracht[3], P.C. Howell[4]

[1] *Faculty Technology and Bionics, Rhein-Waal University for Applied Sciences, 46446 Emmerich, Germany,* Georg.bastian@hochschule-rhein-waal.de

[2] *Institute for Synchrotron Radiation, Karlsruher Institute of Technology, D-76344 Eggenstein-Leopoldshafen, Germany*

[3] *Institut für Materialphysik, Westfälische Wilhelms-Universität Münster, D-48149 Münster, Germany*

[4] *Corporate Research and Technologies, Siemens AG, 81730 München*

Abstract: A new class of phononic metamaterials based on isotopically enriched semiconductor superlattices is presented, which allows tailoring of phononic properties while leaving the electronic properties unaltered. We discuss possible fields of application in thermoelectrics, based on different complementary experimental and theoretical results.

During the last years different techniques have been established to create materials with novel phononic properties. Patterning a material in the nanoscale in one or more dimensions by growth of superlattices or etching techniques are the most common approaches. These structures enable a manipulation of phononic states and a reduced thermal conductivity. However, electronic and photonic transport properties are also negatively affected with this approach. Thermoelectric materials are good examples in which the thermal (phononic) conductivity κ has to be minimized along with a maximized electronic conductivity σ. The figure of merit Z in thermoelectric materials is given by ratio of the conductivities and the Seebeck-coefficient S:

$$Z=\sigma S^2/\kappa \quad (1)$$

Superlattice structures can exhibit an increased ratio although both conductivities are lower than the bulk values[1]. To circumvent this constraint we have investigated isotopically enriched semiconductor superlattices. A single layer consisting of silicon-28 isotope offers an increased phononic mean free path[2]. The slope of the acoustic phonon dispersion relation, i.e. the sound velocity, scales with the square-root of the atom's mass. At an interface between two layers of different isotopes a mismatch of the sound velocities occurs resulting in a small probability of back-reflection, as shown in fig. 1. Multiple interfaces of a superlattice therefore work like a Bragg-grating with an accumulated strong back-reflection, i.e. phononic bandgap.

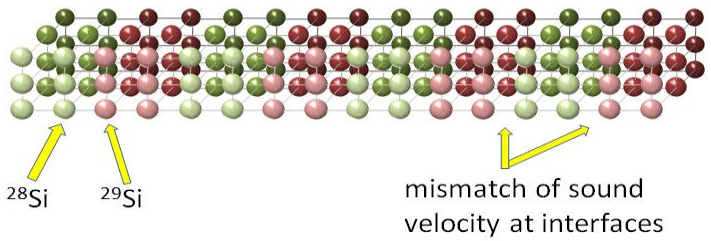

Figure 1 Alternating layers of isotopically enriched semiconductors (Si-28 and Si-29) form a heterostructure for the phonons and a homostructure for the electrons.

In order to verify the concept, different sets of isotopic superlattices made of silicon-28 and silicon-29 have been fabricated. Detailed information of the composition of each layer was gained by depth profiling, as shown in fig. 2. Various methods were applied to determine the thermal conductivity of the multilayer structures. This includes time-domain thermoreflectance, time-resolved X-ray scattering, laser-flash-method, comparative thermal conductivity measurements, and the 3ω–method. Limitations of the classical measurement techniques for thin-film anisotropic materials are discussed. The mea-

Phononics 2011: First International Conference on Phononic Crystals, Metamaterials and Optomechanics
Santa Fe, New Mexico, USA, May 29-June 2, 2011
PHONONICS-2011-0185

surements are compared with results from simulation, including a macroscopic FDTD approach, multiple-interface scattering approximation, and extensive molecular dynamics calculations.

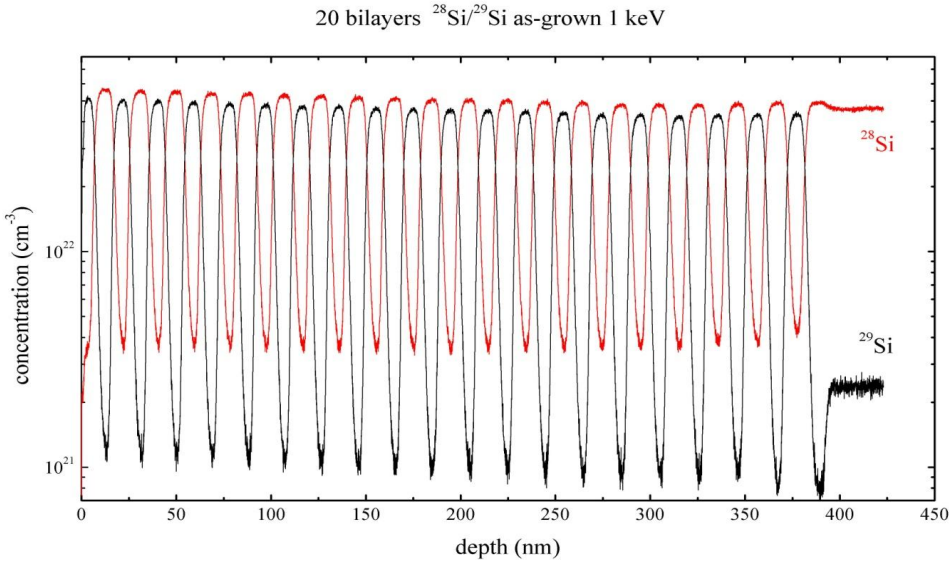

Figure 2 SIMS profiling with a high spatial resolution proves the isotopic composition of the structure: 20 bilayers with a total thickness of 380nm.

Within the uncertainties of the simulations and the uncertainties of the measurements the concept of isotopically enriched superlattices has been demonstrated: A reduction of the thermal conductivity of about 20% for 20 periods of superlattices has been shown. However, there is a limited knowledge about phononic states, anisotropy, coherence lengths, phonon-phonon-scattering and the impact of interface roughness. Therefore, further investigations are required to determine the whole potential of the concept.

References

[1] J. O. Sofo, and G. D. Mahan, *Appl. Phys. Lett.* **65**, 2690 (1994).
[2] T. Ruf, R.W. Henn, M. Asen-Palmer, E. Gmelin, M. Cardona, H.-J. Pohl, G.G. Devyatych, and P.G. Sennikov, Sol. Stat. Comm. **129**, 257 (2003)
[3] A. Plech, V. Kotaidis, S. Grésillon, C. Dahmen and G. von Plessen, Phys. Rev. B **70**, 195423 (2004)